HUMAN PERIPHERAL RETICULOCYTE ISOLATION AND EXOSOME RELEASE IN VITRO

A Dissertation
Presented to
The Academic Faculty

by

Shereka Banton

In Partial Fulfillment
of the Requirements for the Degree
Doctor of Philosophy in the
School of Biomedical Engineering

Georgia Institute of Technology
Emory University
May 2017

HUMAN PERIPHERAL RETICULOCYTE ISOLATION AND EXOSOME RELEASE IN VITRO

Approved by:

Dr. Gilda Barabino, Advisor
School of Biomedical Engineering
Georgia Institute of Technology

Dr. Michael Davis, Co-advisor
School of Biomedical Engineering
Georgia Institute of Technology

Dr. Philip Santangelo
School of Biomedical Engineering
Georgia Institute of Technology

Drs. Betty Pace & Abdullah Kutlar
School of Medicine
Augusta University

Dr. Wilbur Lam
School of Biomedical Engineering
Georgia Institute of Technology

Dr. Lakeshia Taite
Department of Veterinary Pathobiology
Texas A&M University

Date Approved: March 7, 2017

To my family

ACKNOWLEDGEMENTS

I would like to thank my committee for their guidance over the course of this thesis, particularly at the start of my work in 2013-2014 and their help in my laying the theoretical foundation for my research, which I am happy to say was unchanged as I got deeper into the experimental work. Their expertise and insights at the beginning gave me the footing necessary to adjust and adapt my project to the technical and resource constraints that surfaced. I would also like to thank Dr. Kevin Yang, an Associate Research Professor in my lab for his advice and direction at the day-to-day level. Knowing he was coordinating the general operation of the lab freed me to focus on my research. Finally, I'd like to express deep gratitude towards Dr. Gilda Barabino. I have known Dr. Barabino since I was a freshman at Georgia Tech and our relationship, now approaching ten years, has blossomed over the course of this thesis. She gave me the freedom to follow my intellectual pursuits from day one and I am proud to have been able to produce this work under her supervision.

On a personal note, I would like to thank my family and boyfriend for their continued support over the last 5.5 years, particularly with the ups-and-downs of scientific research and my relocation to New York City. Having these individuals as my support system was critical. The completion of this dissertation was a unified effort between my professors, laboratory mates, family, and friends and I give praise to the Highest that this work was done.

TABLE OF CONTENTS

LIST OF TABLES

LIST OF FIGURES

LIST OF SYMBOLS AND ABBREVIATIONS

$\alpha_4\beta_1$	Alpha-4-beta-1 integrin
CD63	Cluster of differentiation 63
CD71	Cluster of differentiation 71
C_T	Cycle threshold number
DMSO	Dimethylsulfoxide
exoELISA	Exosome enzyme-linked immunosorbent assay
FBS	Fetal bovine serum
HUVEC	Human umbilical vein endothelial cell
IL-1β	Interleukin-1-beta
IL-8	Interleukin-8
mRNA	Messenger RNA
miRNA	MicroRNA
PBS	Phosphate buffered saline
qPCR	Quantiative polymerase chain reaction
RIPA Buffer	Radioimmunoprecipitation assay buffer
RBC	Red blood cell, erythrocyte
SCD	Sickle cell disease
HbS	Sickle hemoglobin
Thermo	Thermo Fisher Scientific
TEM	Transmission electron microscopy
TEM	Transmission electron microscopy
TNF-α	Tumor necrosis factor-alpha

VCAM-1	Vascular cell adhesion molecule 1
VEGF	Vascular endothelial growth factor

SUMMARY

The exosomes released by peripheral reticulocytes were originally thought to function as vehicles for protein clearance for the maturing cells. With the emergence of exosomes as mediators of intercellular communication, a new paradigm exists for the role of reticulocyte-derived exosomes in both healthy and disease states, particularly conditions whose pathology is driven by the red blood cell and its precursors. However, no standard or detailed method for the isolation of human peripheral $CD71^+$ reticulocytes exists. A combination of density-dependent and immunomagnetic approaches was used to demonstrate a procedure to isolate human $CD71^+$ reticulocytes from peripheral blood. Nearly 90% of the $CD71^+$ cells were distinct from the $CD71^-$ population when measured with flow cytometry detection of RNA. $CD71^+$ reticulocyte-derived exosomes were then isolated and analyzed after incubation *in* vitro, the first such demonstration of these phenomena using these cells. These findings form the basis for more targeted and mechanistic studies into the role of reticulocyte-derived exosomes in pathologies like sickle cell disease.

CHAPTER 1. INTRODUCTION

1.1 Sickle Cell Disease: A Global Challenge

Sickle cell disease (SCD), the first disorder determined to have a genetic basis, is caused by homozygosity for the mutated β-hemoglobin allele (Pauling, 1949; Barabino, 2010). A point mutation in this allele causes red blood cells (RBCs) to express two sickle β-hemoglobin subunits in each hemoglobin tetramer that polymerize and cause sickling of the RBC in response to deoxygenation. An estimated 300,000 people are born with SCD every year worldwide and 5% of the global population are heterozygous carriers of the sickle β-hemoglobin allele among other hemoglobin disorder variants (World Health Organization, 2014). Moreover, life expectancies are shortened at averages of 42 and 48 years for males and females in the United States, respectively (Platt, 1994). In 2008 the United Nations recognized SCD as a major public health concern because of its rising prevalence globally, particularly in African countries, and concurrent need for better screening, management, and therapies. Hydroxyurea is the only FDA-approved drug indicated to treat the disease, and there exists a substantial need to develop new therapies.

1.2 Reticulocyte-Derived Exosomes, and Sickle Cell Disease

Reticulocytes are immature red blood cells (RBCs) that, like mature RBCs, lack a nucleus. In the 1980s reticulocytes were the first cell type shown to release intracellular materials into nanometer-scale vesicles called exosomes as they develop into mature RBCs and prepare to enter the bloodstream (Pan, 1983; Pan, 1985; Wagner, 1986; Johnstone, 1987). In SCD there are more reticulocytes present in the circulation (Kaul, 1983),

suggesting that conditions are more conducive for these cells to cross the endothelial cell barrier that separates the bone marrow and the bloodstream. Sickle reticulocytes have been shown to have increased surface expression of the α4β1 integrin which is a ligand for the endothelial cell protein vascular cell adhesion molecule 1 (VCAM-1) (Gee, 1995; Styles, 1997). Mature RBCs do not express α4β1. Moreover, sickle reticulocytes have been shown to bind to endothelial cells via α4β1 and VCAM-1 more than mature sickle RBCs. Thus, they are currently thought to initiate vaso-occlusion, or blood flow blockage, in the vasculature by adhering to mature sickle RBCs as well as white blood cells in the circulation which then leads to increased adhesion at the vessel wall and ultimately blood flow blockage (Barabino, 1987; Joneckis, 1993; Swerlick, 1993; Barabino, 2010).

What is unknown is whether exosomes released by reticulocytes package macromolecules—e.g., RNAs or proteins—could be transferred to surrounding cells in a mode of uni- or bidirectional cell-cell communication in both healthy and disease states (Valadi, 2007, Figure 1). Could these reticulocyte-derived exosomes themselves precipate interactions between the endothelial cells that line the vessel wall and the blood cells in the circulation? Moreover, elucidating a possible mechanism of reticulocyte-dependent initiation of vaso-occlusion could ultimately uncover potential points of reticulocyte control that could delay the onset, or reduce the frequency of, vaso-occlusion—essentially stopping the damage to the vessel before it even happens. Therefore, the overarching clinical context of this thesis was moving incrementally towards a reticulocyte-dependent mechanism that may be involved in vaso-occlusion in sickle cell disease, the modulation of which would prevent endothelial cell damage before it occurs during vaso-occlusion.

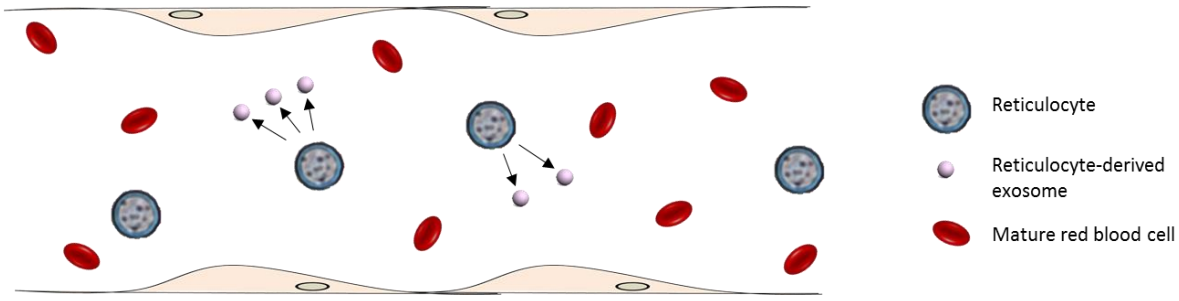

Figure 1 – Schematic of peripheral reticulocytes (image generated in this thesis) releasing exosomes into the peripheral circulation. These exosomes could be internalized by the endothelial cells that line the vessel wall in a mode of cell-cell communication.

1.3 The Need for a Standard Peripheral Reticulocyte Isolation Method

Achieving a reliable approach for isolating reticulocytes from adult peripheral blood is first necessary to investigate the functions of human reticulocyte-derived exosomes in both healthy and disease sates. Peripheral blood, although an obvious and the most accessible source of human reticulocytes, has been supplanted by other blood sources for the isolation of these cells. This has been due to the challenges associated with harvesting usable yields of these cells consistently, given their low numbers—0.5-2.5% of erythrocytes—in the circulation of healthy adults (Kumar, 2015). Consequently, no standard or widely available detailed protocol exists for the isolation of these cells from peripheral blood. For disease states like sickle cell disease, in which the likelihood of reticulocytes being procured from alternative blood sources is low, developing a peripheral reticulocyte isolation method is essential.

Current techniques for the isolation or enrichment of reticulocytes from whole blood are stem cell-based (Giarratana, 2005; Griffiths, 2012, Blood), immunomagnetic (Brun, 1990), or density-dependent (Rushing, 1987; Sorette, 1992; Kumar, 2015). Each technique has its benefits and drawbacks particularly when labor-intensity, cost, and complexity are

considered. Stem cell-based approaches typically require the isolation and long-term culture of $CD34^+$ hematopoietic progenitor stem cells (Griffiths, 2012, Blood). These progenitor cells can be present in the peripheral blood at lower levels than reticulocytes and thus their isolation can also be doubly challenging (Kikuchi-Taura, 2006). Density-dependent approaches, while they can be more labor-intensive, are low-cost, relatively straightforward, and oftentimes do not require any specialized equipment. Immunomagnetic approaches, while more expensive than density-dependent and requiring specialized equipment, offer high specificity for targeted detection of cell surface markers in small samples (< 5mL).

1.4 Specific Aims

The objective of this thesis was to demonstrate and validate a peripheral reticulocyte and reticulocyte-derived exosome isolation approach that is a launching pad for more targeted studies on these cells and their exosomes. This approach is both timely and needed for the continued investigation of reticulocyte maturation and exosome biogenesis. The completion of these aims also offers a new paradigm for the study of diseases states driven by reticulocyte-dependent processes. This project's objective was met with the following specific aims.

1. Specific Aim 1: Establish a protocol for the isolation of $CD71^+$ cells from adult peripheral blood
2. Specific Aim 2: Determine whether $CD71^+$ cells release exosomes *in vitro*
3. Specific Aim 3: Demonstrate that $CD71^+$ cell-derived exosomes can be delivered to endothelial cells

The completion of Aim 1 produced the first widely available, detailed, and visual human peripheral blood reticulocyte isolation protocol, fulfilling a need in the hematology community. Developing this protocol was especially necessary for groups (especially trainees) that need reticulocytes from peripheral blood if no other sources are available. Similarly, the completion of Aim 2 was the first demonstration of exosomes released by human adult peripheral $CD71^+$ cells *in vitro*, the further characterization of which may foster continued study on reticulocyte biology, maturation, and involvement in disease. The completion of Aim 3 will be the first demonstration of $CD71^+$ exosomes being delivered to endothelial cells and the next step of determining *what* is being delivered will be a new direction in the study of reticulocyte-dependent diseases e.g., sickle cell disease.

Overall, this thesis was conceived around the clinical pathology of sickle cell disease and was focused on better understanding the cell at the source of the pathology: the developing red blood cell, specifically the reticulocyte. Through the completion of these aims, the foundation is set to execute studies that delve into both healthy and sickle reticulocyte and reticulocyte-derived exosome function to ultimately develop much-needed therapies. Table 1 provides an overview of this dissertation's organization.

Table 1 – Overview of dissertation.

Chapter	Title	Content
2	Literature Review	Overview of reticulocyte maturation, exosomes, and clinical relevance to sickle cell disease
3	The Isolation of Human Reticulocytes from Peripheral Blood	Studies related to Aim 1
4	$CD71^+$ Cell Release of Exosomes *in vitro*	Studies related to Aim 2
5	Delivery of Exosomes to Endothelial Cells	Studies related to Aim 3
6	Conclusion	Key findings drawn from thesis; future research directions
Appendix	-	Select protocols & R code

CHAPTER 2. LITERATURE REVIEW

2.1 The Clinical Context: Sickle Cell Disease

Sickle cell disease (SCD), the first disorder determined to have a genetic basis, is caused by homozygosity for the mutated β-hemoglobin allele (Pauling, 1949; Barabino, 2010). A point mutation in this allele substitutes a hydrophobic valine for a hydrophilic glutamic acid residue in the β-hemoglobin protein product. Mature red blood cells thus express two sickle β-hemoglobin (HbS) subunits in each hemoglobin tetramer. The presence of the valine residue renders the HbS monomer more prone to hydrophobic interactions between itself and the hydrophobic amino acids in other globin chain subunits. Moreover, HbS polymerization in response to deoxygenation mediates the characteristic sickling of red blood cells in SCD.

It is estimated that 300,000 people are born with SCD worldwide every year and that 5% of the global population (~350 million) are carriers for the sickle gene and thalassemia variants (World Health Organization, 2014). The life expectancies for men and women living with SCD is only 42 and 48 years, respectively (Platt, 1994). Hydroxyurea is the only FDA-approved drug available to treat the disease, and there exists a great need to develop new SCD therapies.

Currently, SCD pathophysiology is categorized into two major processes: vaso-occlusion and hemolysis (Steinberg, 2008; Rees, 2010). Vaso-occlusion in the microvasculature can occur because of sickle red blood cells' reduced deformability inhibiting their ability to flow through the smaller vessels, which can then precipitate the

sickle cell crisis (Ballas, 1992). This localized ischemia, or blockage and reduction of blood flow, can eventually lead to inflammation cascades and infarction in the different organ systems. Some examples are clinical reports of acute chest syndrome, osteonecrosis, and acute pain. Hemolysis is also driven by HbS polymerization. Polymerization can cause red blood cells to lyse, releasing their contents into either blood vessels or surrounding tissue. Hemolysis within the blood vessel can also have an adverse reaction on nitric oxide bioavailability and promote the generation of reactive oxygen species, which can then initiate more inflammatory and white blood cell interaction cascades (Rees, 2010). Ultimately however, SCD's phenotypic profile varies in complexity and severity by patient.

Another clinical manifestation of SCD that is of interest is reticulocytosis, or the increased presence of reticulocytes in the circulations of sickle cell patients (Kaul, 1983). The increased number of reticulocytes in SCD is attributed to the peripheral destruction (hemolysis as described above) of sickle RBCs in circulation in the bone marrow. Peripheral destruction of red blood cells could lead to anemia, the decrease in the normal number of mature RBCs in circulation. The currently presumed compensatory mechanism is an increase in RBC production, which leads to marrow hyperplasia and reticulocytosis, two clinically observed events (Kaul, 1983; Almeida, 2005).

Overall, much is known about hemoglobin polymerization, red blood cell sickling and unsickling cycles and the permanent damage they cause to red blood cell membranes, reticulocytosis, and red blood cell/reticulocyte adhesion to endothelial cells that can precipitate vaso-occlusion in the vasculature—all in the context of SCD (Rees, 2010; Barabino, 2010). However, there is still an overarching and critical need to develop

therapies, which requires exploring new avenues. Investigation of the factors the precipitate the onset of vaso-occlusion—the most common manifestation of the disease—in the microvasculature (capillaries and post-capillary venules) has been an area of concentrated efforts. The current understanding of vaso-occlusion is that reticulocytes initiate the process by adhering to the mature sickle red blood cells as well as white blood cells in circulation. Progressive blockage of blood flow follows (Barabino, 2010).

This thesis uses what is known about cellular interactions in the circulation in SCD and takes an intellectual step back to investigate the source of the pathology: the developing red blood cell, specifically the reticulocyte.

2.2 Reticulocytes

Reticulocytes are the immediate precursor to the erythrocyte, the mature red blood cell. Originating in the bone marrow from erythroid progenitors, reticulocytes lose their nucleus just before entering the peripheral circulation (Ney, 2011). What differentiates reticulocytes from their more mature form is the presence of organelles and residual RNA in their cytoplasms (called reticulum and granules) and their relative size; reticulocytes are 10-15μm in diameter, while erythrocytes are 7-8μm (Riley, 2001). These RNA aggregates and reticulum when stained with an RNA dye are shown in an increasing stage of maturation in Figure 2. Stage 0 represents the reticulocyte precursor (orthochromatic normoblast) prior to enucleation. Stage 1 shows the reticulocyte, now enucleated, with a concentrated area of RNA, likely left over after the enucleation. Stage 2 shows the concentrated RNA area beginning to loosen, signaling increased maturation and the formation of an RNA reticulum network rather than aggregate. Stage 3 shows the increase

in size of the RNA reticulum and Stage 4 shows the remnants of the reticulum once the reticulocyte has reached its most mature form. The consensus currently is that the RNA is gradually lost as the reticulocyte synthesizes the proteins it will need in its mature form. The use of supravital cationic dyes like new methylene blue or brilliant cresyl blue make this type of imaging possible, as the dyes form a noticeable blue precipitate when bound to RNA.

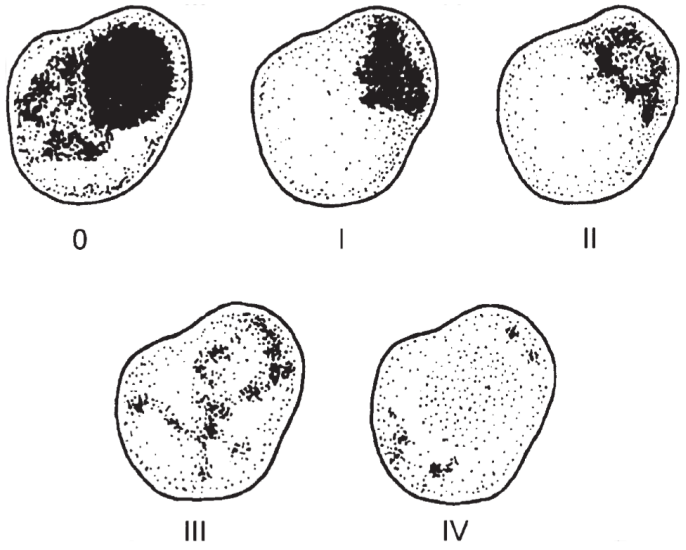

Figure 2 – Representative images of stained reticulocytes durng maturation. The stages are explained in the text. Adapted from Riley, 2001, page 269.

Organelles like mitochondria and ribosomes are also present to support hemoglobin synthesis until they are expelled from the reticulocyte via micron-scale autophagic vesicles as they fully mature (Griffiths, 2012, Autophagy). In healthy individuals, reticulocytes mature over the course of twenty-four hours, a fairly rapid process, and the presence of reticulocytes in the circulation is very low—0.5-2.5% of the mature RBC population (Kumar, 2015). Conversely, in individuals who have hemolytic states (e.g., hemolytic anemias) the presence of reticulocytes in the circulation may increase above normal to

compensate for the inefficiencies in red cell production. Over the course of their maturation, reticulocytes will undergo various processes to assume their mature state: membrane remodeling, organelle clearance, a decline in hemoglobin synthesis until its full hemoglobin complement is reached, changes in metabolic protein expression and finally the focus of this thesis: exosome release of cell membrane protein receptors (Ney, 2001; Riley, 2001).

2.3 Reticulocyte-derived Exosomes

As reticulocytes mature into erythrocytes they package and secrete intracellular components that they no longer need in their mature state into exosomes (Pan, 1983; Harding, 1983; Pan, 1985; Wagner, 1986; Johnstone, 1987; Johnstone, 1991; Blanc, 2005; Johnstone, 2006; Vidal, 2010; Carayon, 2011). Exosomes are vesicles 30-100nm in diameter that originate from multivesicular bodies formed in the reticulocyte's endosomal system. Multivesicular bodies in the cell's endosomal system contain individual exosomes and fuse with the plasma membrane of the cell to initiate exocytosis, after which the exosomes are released into the extracellular space or in more recent years, found to be internalized by neighboring cells in a form of intercellular communication (Figure 3).

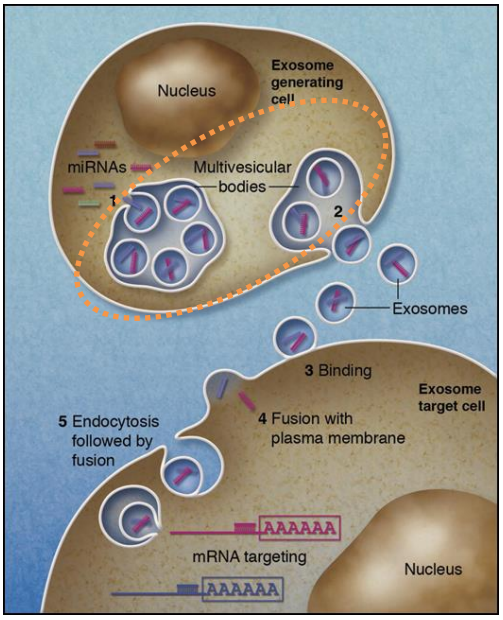

Figure 3 – Multivesicular body origin of exosomes prior to release from a donor cell and internalization by a recipient cell. Adapted from Stoorvogel, 2012, page 646.

Early electron microscopic evidence of exosome release during reticulocyte maturation was reported in the 1980s and serves as the current understanding of exosome biogenesis and release (Pan, 1985; Stoorvogel, 2012). Johnstone et al. found that the exosomes released from sheep reticulocyte culture medium had features characteristic of reticulocytes but absent in erythrocytes, such as transferrin receptor and membrane proteins such as CD55 and CD59 (Johnstone, 1987; Denzer 2000). Figure 4 shows some of the early western blots showing that reticulocytes package the transferrin receptor (94kDa) into exosomes while mature RBCs do not express the protein (Johnstone, 1987). Exosomes are considered critical to transferrin receptor clearance and erythropoiesis in general, because the transferrin receptor was also shown to not be cleared via the lysosomal pathway in reticulocytes. In the case of pathologies whether these exosomes contain other materials is the basis for this thesis, particularly in sickle cell disease whose pathology originates with the red blood cell and its precursors.

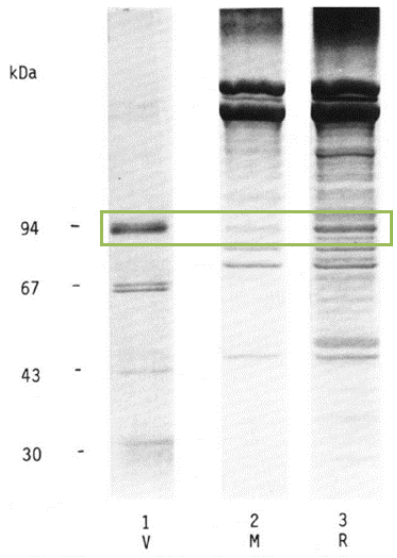

Figure 4 – Early evidence showing that reticulocytes package transferrin receptor (94kDa) into exosomes. Legend: V = vesicles (exosomes), M = mature RBCs, R = sheep reticulocytes. Protein compositions of the plasma membranes of the mature RBCs and reticulocytes are shown, total protein composition in the exosomes shown. Adapted from Johnstone, 1987, page 9414.

Of particular relevance to sickle cell disease is the increased expression of the α4β1 integrin on the membranes of exosomes derived from healthy reticulocytes (Rieu, 2000). The α4β1 integrin is expressed on white blood cells (lymphocytes and monocytes), erythroid progenitor cells, and reticulocytes, but not mature erythrocytes. Moreover, the ligand for α4β1 is vascular cell adhesion molecule (VCAM-1), which promotes leukocyte binding to endothelial cells (Gee, 1995; Styles, 1997). Therefore, the expression of the α4β1 integrin on exosomal membranes suggests two major conclusions: 1) healthy reticulocytes use exosomes to clear the α4β1 integrin from their cell membranes to avoid adverse cell adhesion events and 2) these exosomes could bind to VCAM-1 on endothelial cell surfaces (Rieu, 2000; Denzer, 2000). Sickle reticulocytes have been shown to have increased expression of α4β1; they have also been shown to bind to VCAM-1 via the α4β1 integrin, and therefore endothelial cells, more than mature sickle erythrocytes, which is

why they are thought to initiate vaso-occlusion in the vasculature (Barabino, 1987; Joneckis, 1993; Swerlick, 1993; Gee, 1995; Styles, 1997). Therefore, the expression of the α4β1 integrin on reticulocyte-derived exosomes could further enhance reticulocyte and endothelial cell interactions by enabling more specific binding of reticulocyte-derived exosomes to the target endothelium or may be a factor in the maturation of reticulocytes when they are in circulation. The ultimate role that could play in SCD, or whether it could be exacerbated in some way, is unclear. An initial step could be investigating the expression of the α4β1 integrin on sickle reticulocyte-derived exosomes relative to healthy.

2.4 Human Reticulocyte Isolation and Enrichment Approaches

Understanding the biological action of reticulocytes once they enter the circulation prior to developing into erythrocytes is of considerable interest for links to pathologies where a source of dysfunction may be interactions between RBCs and the vasculature. In sickle cell disease, as mentioned above, chronic hemolysis may lead to the increased presence of reticulocytes in the bloodstream. This suggests a change in the barrier function of the bone marrow endothelium since more reticulocytes are exiting than normal. In addition to their net increase in concentration in the plasma, reticulocytes have been implicated in initiating occlusion in the microvasculature of individuals with sickle cell disease (Barabino, 2010). Therefore, elucidating a new mechanism like exosome-mediated reticulocyte initiation of vaso-occlusion presents a new paradigm for study as well as opportunity for much needed drug modulation. *However, first establishing a systematic and reliable approach for the isolation of peripheral reticulocyte-derived exosomes and their contents is first necessary*.

2.4.1 Density-dependent Approaches

Often, the density differences between reticulocytes, mature RBCs, and leukocytes can be useful to separate the cells. While healthy reticulocytes have a density of 1.084-1.087 g/mL, their mature counterparts have densities greater than 1.087 g/mL and up to 1.1 g/mL (Lew, 2005). Different density gradient media with tunable densities can be used to separate blood components; however, traditionally Percoll, Ficoll, and Histopaque have been used. Percoll, which is a low viscosity fluid containing nano-sized silica particles, can be diluted to a range of densities in isotonic solutions like PBS or NaCl to separate blood components along a specific gradient. 70% Percoll, having a density of 1.09 g/mL, has been used to separate reticulocytes from the red cell fraction (Russell, 2011; Noulin, 2014; Kumar, 2015). Similarly, these density gradient media can be used to remove leukocytes when red cells are the desired cell type for investigation. Ficoll and Histopaque, both polysaccharide-based solutions, are typically used to enrich peripheral blood mononuclear cells from whole blood and have been shown to deplete blood of leukocytes en route to reticulocyte enrichment (Chen, 2008). However, because the density of commercially available Ficoll and Histopaque is 1.077-1.078 g/mL, the separation of reticulocytes from whole blood prior to any leukocyte removal can be challenging because granulocytes will also be enriched with the reticulocyte population; e.g., the density of neutrophil, the most abundant granulocyte, is greater than 1.08 g/mL (Zucker 1969). Recently, aqueous multiphase polymers have also been introduced as a tool for reticulocyte isolation from peripheral blood (Kumar, 2015). The two-phase hypertonic system is made by layering of equal weight-by-volume percentages of dextran and Ficoll, so also polysaccharide-based, and reticulocytes can be enriched from leukocyte-depleted blood

with centrifugation after layering it over the multiphase system. The challenge of adapting this approach would be around the synthesis of these multiphase polymers in labs that do not have that particular expertise.

The major advantage to using density gradient media is that these solutions are nontoxic to cells, easy to dilute and tune their densities, and highly stable (e.g., Percoll is stable from 4ºC up to room temperature), and easy to remove from the solution once the desired cells are collected. Moreover, once sample preparation is well thought-out, the execution of these separation steps only requires mastering the gentle layering blood on top of the gradient and a standard benchtop centrifuge with a swinging bucket rotor. The total time of the centrifugation runs, depending on the number of runs and sample preparation step needed can however, make the process very time- and labor-intensive.

2.4.2 Immunomagnetic Approaches

Immunomagnetic approaches allow investigators to target specific membrane markers on the reticulocyte surface. The traditional marker is CD71, which is the transferrin receptor (Brun, 1990). While reticulocytes mature in the circulation, the transferrin receptor transports iron into the maturing cell to aid in hemoglobin synthesis. As the reticulocyte reaches it full haemoglobin complement, it no longer needs the transferrin receptor and exocytoses it via exosomes (Pan, 1983; Riley, 2001). Thus, mature RBCS do not express CD71 on their membranes and this distinct expression profile between reticulocytes and mature RBCs can be used to separate the cells from blood (Brun, 1990; Chen, 2008; Malleret, 2015; Cho, 2016). Similarly with density-dependent approaches, an initial leukocyte depletion step is needed because circulating leukocytes

also express CD71 (Ponka, 1999). Leukocyte removal can be done with another marker for leukocytes to exclude those cells (e.g., CD45 by Chen et al. in 2008) or with a filtration step using cellulose columns for example (Russell, 2011; Noulin, 2014; Cho, 2016).

The high specificity for the CD71 marker, among others, makes immunomagnetic approaches very attractive. Particularly, in automated separator like the AutoMACs cell separator manufactured by Miltenyi, these separations can be done in under five minutes. However, magnetic beads can be pricey and often most applications for blood separation would require a considerable number of beads without any pre-purification steps. For example, 1mL of blood contains on average contains 4-6 billion red blood cells alone. The capacity for the autoMACs cell separator is up to 10^9 cells per run. If one collects a 5mL sample, then a pre-processing step would be necessary to bring down the total number of cells due to the machine's upper cell limit and to increase the yield of the targeted cell, in this case the reticulocyte. Moreover, a pre-purification step is even more crucial for healthy samples, in which reticulocytes are only 0.5-2.5% of the mature RBC population. Given the costs associated with this approach, maximizing the potential for usable yields of reticulocytes is very important. Of course, the alternative is sacrificing some percentage of the sample in order to limit the amount of magnetic beads used in individual runs.

2.4.3 Stem Cell Approaches

A consideration in studies investigating reticulocyte maturation is the stage of maturation of isolated peripheral reticulocytes and how relevant *in vitro* analysis of their macromolecule content would be if they have already exited the bone marrow. To address this concern, investigators often turn to $CD34^+$ cells from the peripheral blood which can

then be cultured *in vitro* until enucleation. Of note is that $CD71^+$ (transferrin receptor-expressing) cells isolated from the peripheral blood are considered "young" reticulocytes (Skadberg, 2003). Starting with a progenitor cell less mature than the peripheral reticulocyte may be more applicable hypotheses about reticulocyte maturation, and erythropoiesis in general.

CD34 is a glycoprotein expressed on hematopoietic progenitor cells and these cells can be directed towards terminal erythroid differentiation and mature into enucleated cells (reticulocytes & erythrocytes) after culture *in vitro* (Douay, 2009; Sangokoya, 2010; Griffiths 2012, Blood; Hu, 2013). Moreover, these cells have been shown to be viable in vivo (Giarratana, 2011). Griffiths et al. have shown the differentiation timing for $CD34^+$ cells *in vitro* as they mature into erythrocytes (Figure 5). Figure 5 shows that over the course of a 20-day culture period the percentage of reticulocytes increases slowly after days 10-11. After day 20 a leukocyte filter was used to separate the more mature reticulocytes (closer in phenotype to erythrocytes) from the rest of the cells in cultures (Griffiths, 2012, Blood). Leukocyte filters take advantage of the negative surface charges on leukocytes and mature reticulocytes/erythrocytes by promoting the adhesion of those cells to the filter material (Sharma, 2010). The overall advantage of this method is the enhanced control of cell maturation. However, cell yields, the technical difficulty in stem cell differentiation and long-term cultures, and the expense of differentiation medium can make this approach particularly challenging.

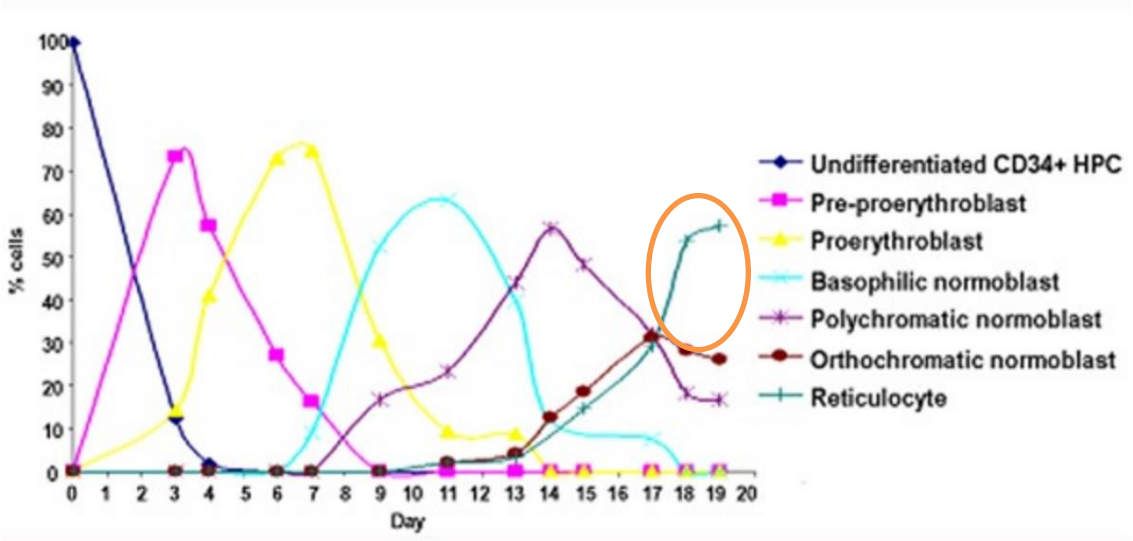

Figure 5 – Percentages of erythroid precursors during 20-day *in vitro* erythroid differentiation culture. The percentage of reticulocytes (orange circle) increases slowly after days 10-11 and by day 20 is the most abundant cell type signaling the shift of the system towards terminal erythoid differentiation. Adapted from Griffiths, 2012, Blood, page 6298.

2.4.4 Final Summary of Reticulocyte Isolation Approaches

Table 2 summarizes the approaches detailed above. It is worth noting that these approaches can be combined, as in presented in this thesis (Chapter 3). No one approach is necessarily better than the others, but the factors listed into the table should be considered when determining the best direction. As far as innovation in this area, there exists need for newer techniques for the isolation of reticulocytes from peripheral or other blood sources. In the age of labs on a chip and microfluidic devices, whether these approaches could be scaled to that size is an interesting possibility, especially considering the engineering design that would be necessary. However, the wide access and availability of a standard, even if laborious, approach is the first step towards driving that innovation because innovators always need some starting point (of unmet need) from which to draw inspiration.

Table 2 – Summary of major reticulocyte isolation approaches.

Approach	Pros	Cons
Density-dependent	Cheap No specialized equipment	Time- and labor-intensive Possible mixing of non-target cells Require leukocyte depletion step
Immunomagnetic	High specificity If automated: very fast	Relatively expensive Requires specialized equipment Requires pre-purification steps to minimize bead volume
Stem cell	Granular analysis of cells during maturation	Long-term cultures Variability in differentiation profiles Availability of stem cells

2.4.5 Reticulocyte Isolation Approach Chosen to Begin Execution of Aims

Table 3 shows select reticulocyte isolation or enrichment approaches that were evaluated prior to the choosing of an approach for the execution of this thesis' aims.

Table 3 – Evaluation of select reticulocyte isolation approaches. DD = density-dependent, I = immunomagnetic.

Author	Blood Source	Isolation Method (DD, I)	Additional information
Russell, 2011	Cord	DD (Percoll); from red cell fraction	Enrichment of cells
Miltenyi rep, 2013	Peripheral	DD (Histopaque); from PBMC fraction	PBMCs in cell mixture
Kumar, 2015	Peripheral	DD (multiphase polymers)	Requires synthesis of polymers
Cho, 2016	Cord	I; from red cell fraction	Reagant (magnetic bead) volume not reported
Other	Human or animal; cord or peripheral	DD and/or I	Sample and reagent volumes, cell yields often not reported

The approaches were evaluated according to the following criteria: 1) level of straightforwardness, 2) financial expense, 3) level of detail in published article's methodology, and 4) level of adaptability. These criteria were not weighted. The "Other" category captures other references that are not specified in the table, but read during a survey of the literature (Johnstone, 1987, sheep; Rieu, 2000, rats and non-leukocyte-depleted human blood, Koury, 2005, mice; Blanc, 2007, rats; Chen, 2008, packed human erythrocyte pellet; Blanc, 2009, mice; Barrès, 2010, rats; Liu, 2010, mice; Martin-Jualar, 2011, mice and non-leukocyte-depleted blood; Noulin, 2014, stem cells; Malleret, 2015, 25µL cord blood). Generally, these approaches entailed the use of either animal or human peripheral or cord blood with varying permutations of the major isolation approaches. Cord blood, since it has a higher percentage of reticulocytes than peripheral blood, is also considered a better source for reticulocytes for malaria parasite invasion studies (Moreno-Pérez, 2013). Furthermore, neither sample and reagent volumes nor cell yields were reported in a way that made the adaptability of these methodologies possible. This speaks to the need in the literature for a very detailed and graphically-supported approach for reticulocyte isolation from peripheral blood, one that once mastered can spur further innovation. The Miltenyi representative field is anecdotal. Consultation with a sales representative from the manufacturer of the automated immunomagnetic cell separator resulted in the exchange of a protocol for the isolation of $CD71^+$ cells using Histopaque. However, the challenge faced with that protocol was the inclusion of peripheral blood mononuclear cells, specifically granulocytes, in the reticulocyte-enriched mixture. The presence of these cells was not desirable because of their potential to release exosomes (Hunter, 2008).

When the four criteria were considered, the Russell, 2011 methodology was selected primarily because of its more detailed and adaptable methodology. Additionally, since the technique is density-dependent no special equipment was required. The use of cord blood in that study did not cause any concern because the density difference between the reticulocytes and the mature RBCs was not expected to be different based on the blood source. Moreover, peripheral blood was more available for the execution of this project while cord blood was not. Conversely, the Kumar, 2015 approach, while novel, required the synthesis of the aqueous multiphase polymers, an expertise not currently in-house. The CD71 magnetic bead volume used was not specified in the Cho, 2016 approach which is critical given the expense of the beads. Additionally, their use of 1-2mL of cord blood may have been sufficient given the low reticulocyte level in that blood source; their reticulocyte yield was not reported. However; that volume from peripheral blood may not have resulted in desirable yields of reticulocytes for the purposes of this thesis and the retrieval of exosomes.

2.5 Exosomal Communication via Macromolecules: A Spotlight on MiRNAs

Mature microRNAS (miRNAs) are small, approximately 20 nucleotide-long molecules that are involved in the regulation of protein expression in cells (Davidson, 2011). miRNAs can act to repress the start of translation by inhibiting ribosomal traversing of messenger RNA (mRNA) transcripts. MiRNAs can also act to degrade their target mRNAs by initiating the shuttling of the mRNAs to intercellular processing bodies where mRNAs are either stored or degraded. Through either mechanism, the net result is reduced translation of the target mRNA transcript and thus, protein expression. The role of miRNAs in cardiovascular diseases, including SCD, is still being uncovered (Latronico,

2007; Small, 2011; Hata, 2013). MiRNAs serve as a new paradigm within which to approach investigation into pathologies like sickle cell disease because of the diverse functional effects they can have on protein expression and whether those effects are aberrant in the disease state.

Chen et al. have shown that the expression of specific miRNAs in sickle erythrocytes is markedly different than in healthy ones (Chen, 2008). Figure 6 shows that healthy, but not sickle, reticulocytes and erythrocytes have different miRNA expression profiles, which implies that the different miRNAs expressed may impose different functional effects on the reticulocytes, RBCs, and even cells in their extracellular environments. Whether there are differences in miRNA expression profiles between sickle and healthy reticulocytes and their functional effects is unknown.

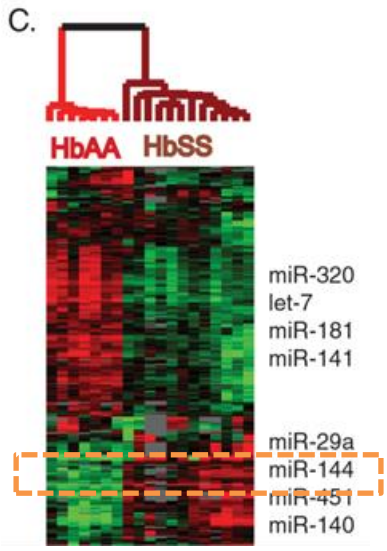

Figure 6 – MiRNA profiles differ in sickle and healthy erythrocytes. miR-144 is expressed more in sickle erythrocytes than in healthy erythrocytes. Adapted from Chen, 2008, page e2360.

Chen et al. also demonstrated that miR-144, miR-29a, miR-451, and miR-140 are expressed more in sickle erythrocytes than in healthy erythrocytes. A small focal point of this thesis is miR-144, which is an erythroid lineage-specific miRNA (Bonauer, 2010; Latronico, 2007). MiR-144 has been implicated in controlling erythroid cell development and homeostasis and its allele has been demonstrated to be a reliable marker for erythroid differentiation tracking in vivo (Rasmussen, 2010; Rasmussen, 2011). MiR-144 levels in sickle reticulocytes have been correlated positively to the severity of anemia in sickle patients as measured by patient hematocrits and plasma hemoglobin counts (Sangokoya, 2010). This evidence makes it a suitable focal miRNA.

Additionally, cells can "communicate" with each other via their miRNA-containing exosomes *in vitro* (Valadi, 2007; Zhang, 2010; Kosaka, 2010; Ramachandran, 2011; Stoorvogel, 2012; Hergenreider, 2012). Generally, in this scenario an exosome-donating cell secretes and directs its exosome to a recipient cell, where the miRNAs packaged in the exosomes exert functional effects on the recipient cell (Figure 3). Given that reticulocytes have been observed to exocytose different intercellular components that are not required by the mature red blood cell via exosomes, there is the possibility that within these exosomes are miRNAs that serve as intercellular signaling molecules. This suggests a more defined functional role for exosomes beyond the selective packaging of intracellular materials reticulocytes do not need as they are maturing. In SCD, the role of miRNAs in reticulocyte maturation and exosomal release has not been investigated extensively beyond the differential expression profiles in sickle erythrocytes and their precursors and the effects of specific miRNAs on oxidative stress capacity (Chen, 2008; Sangokoya, 2010).

CHAPTER 3. THE ISOLATION OF HUMAN RETICULOCYTES FROM PERIPHERAL BLOOD

3.1 Introduction

Reticulocytes in peripheral blood are a heterogeneous population of cells that differ based on the stage of their maturation into erythrocytes. Figure 7 shows the range of densities and hemoglobin levels along which both healthy and sickle red blood cells exist in humans. Reticulocytes, with greater cell volume and lesser hemoglobin content than mature RBCs, have lower densities with an average value of 1.084-1.087 g/cm^3 for normal reticulocytes. As Figure 7 shows, sickle reticulocytes can have densities less than 1.06 g/cm^3. Separating RBC populations according to this granular density difference is ideal in cases when reticulocytes are needed for investigation. For the reticulocyte isolation method reported in this chapter 70% Percoll, the density of which is equal to 1.09 g/cm^3, was used to enrich reticulocytes from leukocyte- and platelet-depleted blood (Russell, 2011).

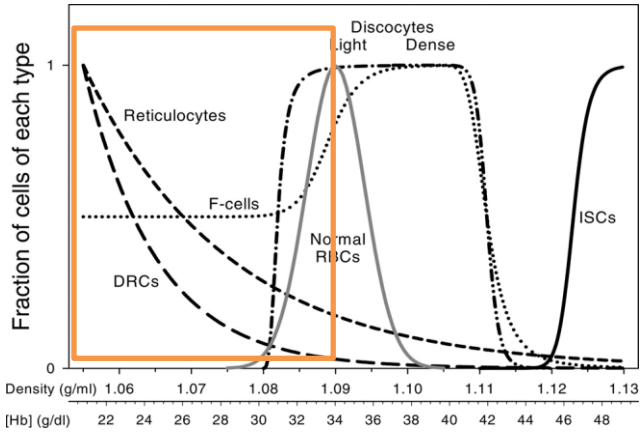

Figure 7 – Density and hemoglobin profiles for normal and sickle RBCs. Adapted from Lew, 2005, Physical Reviews, page 182.

Similarly, taking advantage of the differential expression of protein markers on the surfaces of mature RBCs and their precursors with antibody-based products is also a useful technique for enriching or purifying specific subpopulations of cells out of a larger population. CD71, the transferrin receptor is a membrane protein critical for iron transport in maturing RBCs and its expression level on the cells is an indication of red blood cell maturation (Skadberg, 2003). CD71 is a iron transporter that shuttles the metal into maturing red blood cells to support hemoglobin production. As reticulocytes mature, their membrane CD71 expression decreases, indicating the cells have reached the maximum hemoglobin content needed for their lifespan. Therefore, mature RBCs do not express CD71 (Sieff, 1982; Skadberg, 2003).

For this thesis, achieving a reproducible approach for isolating reticulocytes from peripheral blood was necessary despite the blood source's low reticulocyte count. The reported method drew from a previous approach (Russell, 2011) for reticulocyte enrichment from cord blood was performed, now with the use of peripheral blood. This method utilizes both density-dependent (Percoll) and immunomagnetic (CD71 positive selection) approaches, generally described in Chapter 2. Validation of the separation was performed with flow cytometry and cytological staining detection of RNA because reticulocytes also package RNA into granules to complete protein production without a nucleus while maturing in the circulation (Griffiths, 2012, Autophagy). This chapter will demonstrate a stepwise progression of the established approach, while providing a detailed methodology. As no standardized protocol exists for the isolation of human peripheral reticulocytes from whole blood, the steps described here will fill that gap in knowledge. A

chart of the separation process is shown in Figure 8, the images and the steps of which are detailed in the Materials and Methods section.

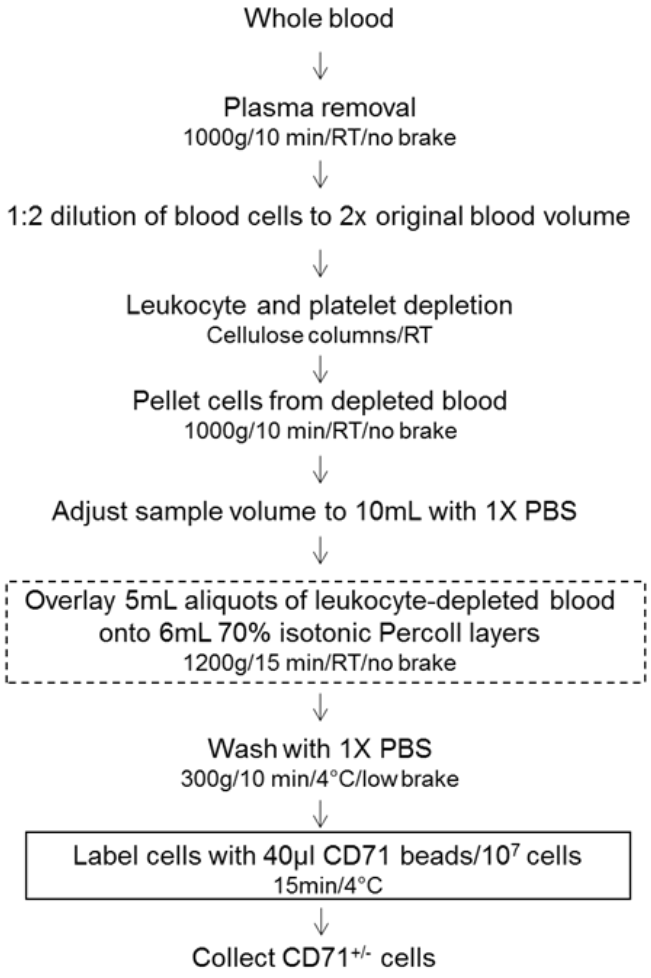

Figure 8 – CD71$^+$ cells can be isolated from peripheral blood using density-dependent and immunomagnetic approaches. (A) The workflow. The box with a dashed outline indicates the 70% Percoll density-dependent separation step, while the box with a solid outline indicates the immunomagnetic separation step.

3.2 Materials and Methods

3.2.1 Blood Sample Collection

Human whole blood (10mL) from healthy adult African-American donors was purchased from an institutional IRB-approved commercial vendor, Research Blood

Components (Boston, MA). The 10mL blood samples were collected over EDTA and guaranteed to be syphilis–, HTLV–, HIV–, HepB–, and HepC–. Reticulocytes were isolated from all samples within twenty fours of being collected.

3.2.2 Cellulose Column Preparation

Cellulose columns (Figure 9) were used to deplete white blood cells and platelets from peripheral red blood cells (Venkatesan, 2012). First, two 1 cm^2 squares of lens paper (Whatman) were laid flat to cover the tip of a 10mL Luer-Lok syringe (BD). The syringes were then packed with 5.7 mL of cellulose powder (Sigma-Aldrich) and stored at room temperature prior to use.

Figure 9 – Cellulose column used to deplete leukocytes and platelets from blood. 10mL syringes were packed with 5.7mL cellulose on the day prior to reticulocyte isolation.

3.2.3 70% Isotonic Percoll Solution Preparation

"100%" Percoll was prepared by adding nine parts cell-culture tested Percoll (Sigma-Aldrich) to one part 10X PBS. 70% isotonic Percoll was then prepared by diluting the "100%" Percoll with 1X PBS (Frank, 2006). The density of the 70% Percoll solution was approximately 1.09 g/mL based on the manufacturer's specifications for density calculations and the diluents used. The solution was brought to room temperature prior to use.

3.2.4 Enrichment of Reticulocytes from Blood With 70% Percoll

Centrifugation for ten minutes at 1000g was first used to remove plasma from the blood samples. After plasma removal, the packed cells were diluted to twice the original blood volume in 1X PBS. White blood cells and platelets were depleted from the peripheral red blood cells using the cellulose columns described above (Figure 10).

Figure 10 – Blood undergoing leukocyte and platelet depletion in cellulose columns.

The columns were first hydrated with 6mL 1X PBS, then loaded with 5mL of the diluted blood. After the blood passed through the columns, 5mL 1X PBS was added to wash the columns. After the wash, the leukocyte- and platelet-depleted blood was centrifuged for 10 minutes at 1000g and the total volume of the sample brought to 10mL. 5mL aliquots were then gently overlaid on 6mL 70% Percoll layers in 15mL conical tubes using the gravity mode dispense setting on a motorized pipettor (Figure 11). All centrifugation runs in this stage were done at room temperature in a swinging bucket rotor and without brakes.

Figure 11 – Demonstration of layering blood over 70% Percoll cushion without any mixing or disruption of the interface (6mL mark on tube) between the two media.

3.2.5 Immunomagnetic Selection of CD71$^+$ Cells from Percoll-Separated Blood

Three distinct layers were observed above the Percoll cushion after 70% Percoll separation. The bands were carefully removed using a micropipettor, pooled, and washed

in 1X PBS. Cells were pelleted by centrifugation for 10 minutes at 300g and 4°C. After the post-Percoll separation wash the cell pellet was resuspended in 1X PBS and the total number of cells quantified with the Countess II (Life Technologies) automated cell counter.

The cells were then resuspended in 80µl autoMACS separation buffer (Miltenyi, 1X PBS/0.5%BSA/2mM EDTA) per 10^7 cells and treated with 40µl of human CD71 microbeads (Miltenyi) per 10^7 cells for 15 minutes at 4°C in the dark. After the incubation time, the cells were washed with 1mL of separation buffer per 10^7 cells, centrifuged, and resuspended in 500µl of separation buffer. $CD71^+$ cells were then isolated using the positive selection program on the autoMACS separator (Miltenyi). $CD71^-$ cells were also collected. Both cell populations were resuspended in 1X PBS and stored at 4°C until further use. All centrifugation runs in this stage were completed at 400g and 4°C for 5 minutes in a swinging bucket rotor and with low deceleration, unless otherwise stated.

3.2.6 Flow Cytometry for Acridine Orange-Bound RNA Detection

To detect the RNA content in $CD71^{+/-}$ cells, 250,000-500,000 cells in each sample were incubated with 10µg acridine orange (ThermoFisher Scientific) for 30 minutes at room temperature. Fluorescence of acridine orange-bound RNA (10,000 events) using the LSR II 4 flow cytometer (BD Biosciences) was recorded immediately after incubation. A one-tailed, unequal variance, 97.5% confidence level student's independent t-test was performed to compare the mean acridine orange fluorescence between the $CD71^{+/-}$ populations and to evaluate the effectiveness of the combined density-dependent and immunomagnetic separation steps. Prior to running the t-test a 95% confidence level F-test was used to test whether the variances of the populations were equal or unequal. P-

values less than 0.025 were considered indicative of a statistically significant result. Equation 1 shows the formula used to calculate the effect size (Cohen's d) as another measure of the difference between the means.

$$Cohens'd = \frac{\left|\mu_{population1} - u_{population2}\right|}{SD_{pooled}} \quad (1)$$

To account for differing sample sizes, a pooled standard deviation was used in the calculation of effect size. The formula for the pooled standard deviation is in Equation 2. All analyses were done in R or Excel.

$$SD_{pooled} = \sqrt{\frac{(n_1 - 1)SD_1^2 + (n_2 - 1)SD_2^2}{n_1 + n_2 - 2}} \quad (2)$$

3.2.7 Brilliant Cresyl Blue RNA Staining

250,000 $CD71^{+/-}$ cells were stained 1:1 with a 1:100 dilution of the live-cell RNA stain brilliant cresyl blue (EMD Millipore) for thirty minutes (Noulin, 2014). After the addition of 300-400µl warm culture medium (see exosome isolation section), the solution was spun in the Cytospin cytocentrifuge (ThermoFisher Scientific) for three minutes at 700rpm with low acceleration. Slides were air dried prior to imaging.

3.3 Results & Discussion

3.3.1 Detection of Three Discrete Bands Above the 70% Percoll Cushion

The image on the right of Figure 12 shows the first successful 70% Percoll separation that was performed with human peripheral blood with the Russell, 2011 approach. The image on the left side of Figure 12 shows the 70% Percoll separation result with cord blood that was reported by Russell et al. in 2011. The two black arrows indicate what were thought to be the primary reticulocyte-containing band in each sample. However, when the peripheral blood separated sample was inspected more closely, there appeared to be more than one layer—actually three in total, with one above and below the primary band. To determine whether the cells were reticulated, the uppermost two bands of the peripheral blood sample in Figure 12 were aspirated and stained with brilliant cresyl blue. Similarly, the third layer was also stained to determine whether reticulated cells were present. Reticulated cells were detected in all layers (Figure 13 and Figure 14).

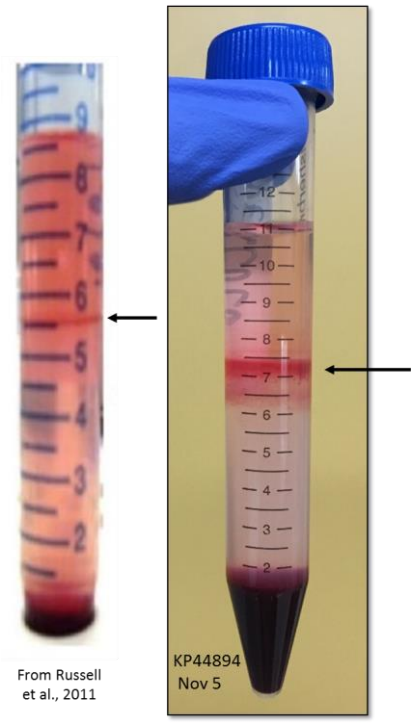

Figure 12 – Comparison of 70% Percoll separation results with cord (left, adapted from Russell, 2011, page e76) and peripheral (right) blood.

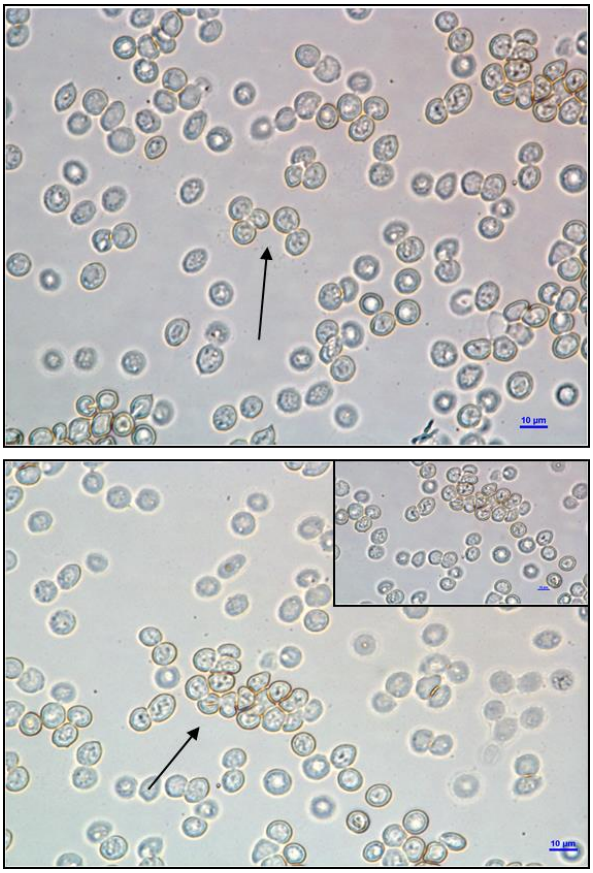

Figure 13 – Brilliant cresyl blue staining of uppermost two layers post-Percoll. Scale bars: 10µm.

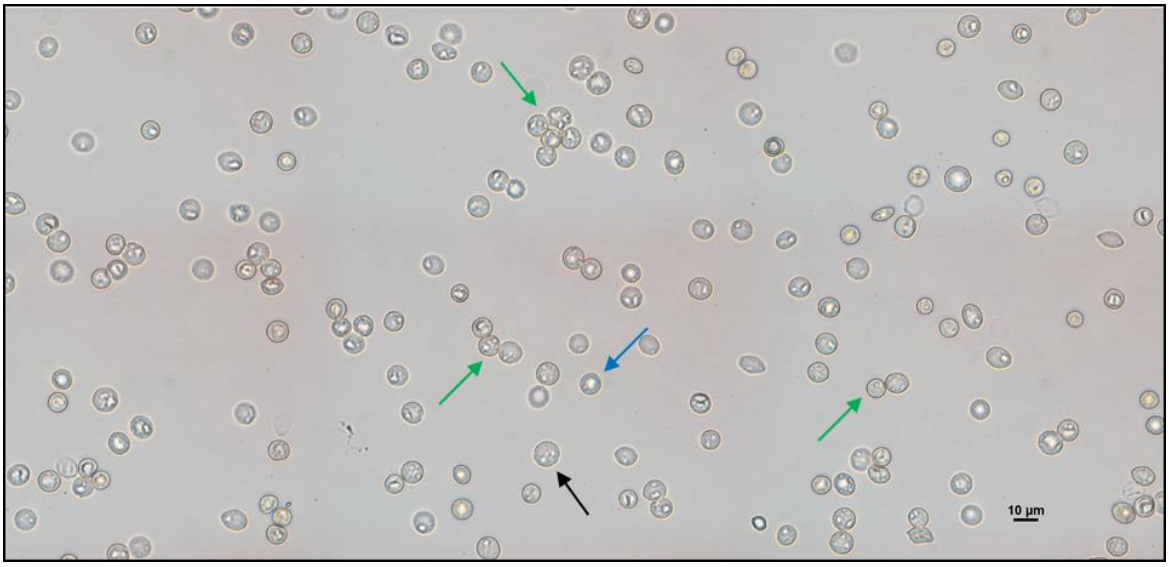

Figure 14 – Cells detected in the lowest band. Green arrow: reticulated cells; black arrow: larger cells; blue arrow: most mature cell. Scale bar: 10µm.

In Figure 14 reticulated cells detected in the lowest band are shown. Three different cell morphologies are highlighted. First, cells that had sparsely reticulated cytoplasms, those with interchanging areas of white and blue are highlighted with the green arrow. These are reticulocytes, akin to the cell shown in Stage 4 of Figure 2. Cells with a region of central pallor (whiteness) are highlighted by the blue arrow. These cells are likely newly mature RBCs and again akin to Stage 4 of Figure 2—or right after, although their density is below 1.09 g/mL. Finally, cells slightly larger than the others are indicated by the black arrow. These may be cells that have yet to expel their organelles and undergo membrane organization as they become mature RBCs. Taken together, these results led to the conclusion that three discrete layers were being observed after 70% Percoll separation of peripheral blood (Figure 15). Given the density-dependent nature of this method, general properties of the individual layers were defined with respect to their relative densities and reticulocyte maturation (Lew, 2005). Layer 1, the uppermost layer, is thought to contain the youngest (least dense) reticulocytes, the middle band relatively older reticulocytes, and the lowest band the densest cells—the oldest reticulocytes and newly mature erythrocytes. Further study on the individual layers could provide clarification. Additionally, only one reticulocyte-containing band was previously reported in similar approaches (Figure 12; Russell, 2011; Kumar, 2015). This could be due to the compositional differences of the cord blood that was used in one of the studies or to overall differences in technique. No reports of three layers being observed were found in the literature, a result that was quite remarkable.

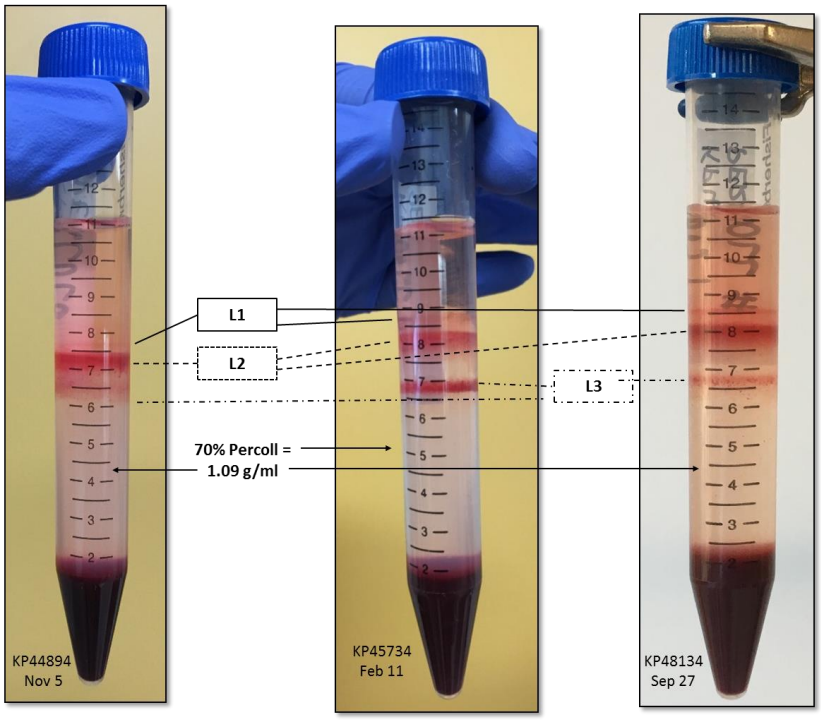

Figure 15 – Confirmation of three layers being detected. L = layer.

3.3.2 CD71$^+$ Immunomagnetic Separation of the Pooled Three Layers

The three bands observed after Percoll isolation were pooled and underwent CD71$^+$ immunomagnetic selection. The mean number of CD71$^+$ cells that were isolated from eleven 10mL samples of healthy peripheral blood was $2.47 \times 10^6 \pm 7.49 \times 10^5$ cells (Figure 16). CD71$^+$ cell yields varied across donors and may reflect their different steady-state peripheral reticulocyte levels, which were expected to be low since the donors were not anemic. We did not observe any age or gender trends in the number of CD71$^+$ cells isolated. Table 4 summarizes this data as well as the ratio of CD71$^+$ cells collected to the total number of cells that were collected after 70% Percoll separation. The mean ratio was 2.19% ± 0.412%. This indicates that when combined with 70% Percoll enrichment of reticulocytes, CD71 immunomagnetic separation of the youngest reticulocytes (Skadberg, 2003) further purifies the population. However, the CD71$^-$ population, representing the

other ~98%, may be sufficient for some investigations because the density of these cells is still below 1.09 g/mL and in the range of commonly accepted reticulocyte densities (Lew, 2005). A possible deterrent to the use of this population would be the high total cell count, a value that would approach $100x10^6$ cells. The same applies with stopping at the 70% Percoll separation step and collecting the cells from the pooled layers (average of $106x10^6$ cells). On the other hand, the concentration of beads used may set an upper limit on the number of $CD71^+$ cells that can be collected from one sample. This work's treatment concentration of 40µl beads/10^7 cells may set an upper limit across the samples, and in fact some cells in the $CD71^-$ population could be unlabeled, yet $CD71^+$ cells. In any case, what is considered an acceptable number of $CD71^+$ cells is left to the preferences of the individual researcher.

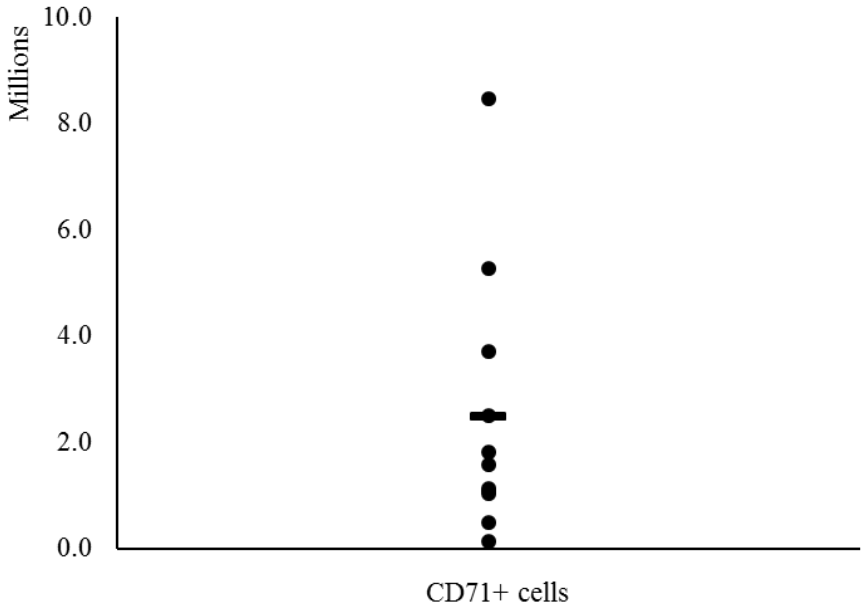

Figure 16 – The number of $CD71^+$ reticulocytes isolated varied across the healthy donors (n=11). The number of $CD71^+$ reticulocytes were quantified after immunomagnetic selection. A mean of $2.47x10^6 \pm 7.49x10^5$ $CD71^+$ cells were isolated from the 10mL samples; 95% confidence interval: ($1.0x10^6$, $3.94x10^6$). The horizontal bar represents the mean cell number.

Table 4 – Summary of CD71$^+$ yields per donor (n=11).

Sample ID	# of CD71$^+$ cells (x10^6)	# of cells post-Percoll (x10^6)	Ratio (%)
KP48474	1.13	50.0	2.25
KP48511	1.03	30.0	3.43
KP48556	1.08	97.5	1.10
KP48599	0.132	66.8	0.198
KP48635	1.82	74.4	2.44
KP48660	5.27	109	4.84
KP48773	0.481	68.0	0.708
KP48903	2.49	168	1.49
KP48934	1.58	110	1.43
KP49050	8.45	277	3.05
KP49112	3.72	119	3.11
Mean	2.47	106	2.19
SEM	0.749	20.5	0.412

3.3.3 Flow Cytometry Detection of RNA in CD71$^{+/-}$ Cells

3.3.3.1 Acridine Orange Staining of CD71$^+$ Cells

Flow cytometry detection of acridine orange-stained RNA in CD71$^+$ cells further detected the presence of RNA in these cells (Figure 17). When acridine orange fluorescence in stained and unstained CD71$^+$ cells were compared, a shift in the peak fluorescence between the two populations was evident when a gate was drawn from the right edge of the unstained histogram to the extent of the x-axis (Figure 17, third panel). The drawing of this gate in the analysis software was done manually. Additionally, the forward scatter vs side scatter plots on a linear scale are shown in Figure 17. Notice that acridine orange, at a treatment amount of 10µg, led to the reduced side scatter and increased

forward scatter of the stained CD71^{+} cells. RNA granules ("particulates") may contribute to reticulocyte granularity such that when the flow cytometer laser contacts the cell it may be bouncing off the RNA in the cell. Acridine orange binding the RNA may then reduce the granularity if the RNA is complexed with the dye. For the increase in forward scatter which is a proxy for cell size, the uptake of the acridine orange may lead to an increase in cell volume of the reticulocytes, which since they have few organelles and no nucleus, may have the acridine orange forming structures in their cytoplasms that lead to a slight increase in cell size (Jahanmehr, 1987). Overall, these data indicate that RNA was detected in the acridine orange-treated CD71^{+} cells.

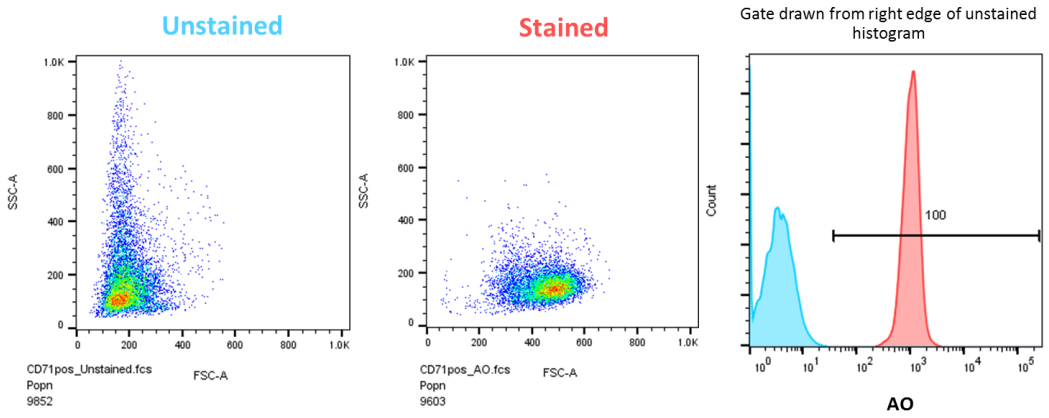

Figure 17 – Flow cytometry detection of RNA in CD71^{+} cells using acridine orange.

3.3.3.2 Comparing CD71$^{+/-}$ Stained Cells

The motivation for comparing the stained CD71$^{+/-}$ cells was derived from analysis of the six unstained and stained CD71^{+} samples (Figure 18). Notice that in the box labeled KP48599 that the percentage of CD71^{+} stained cells that were unique from the CD71^{+} unstained cells was 65.9%, a value lower than the other samples.

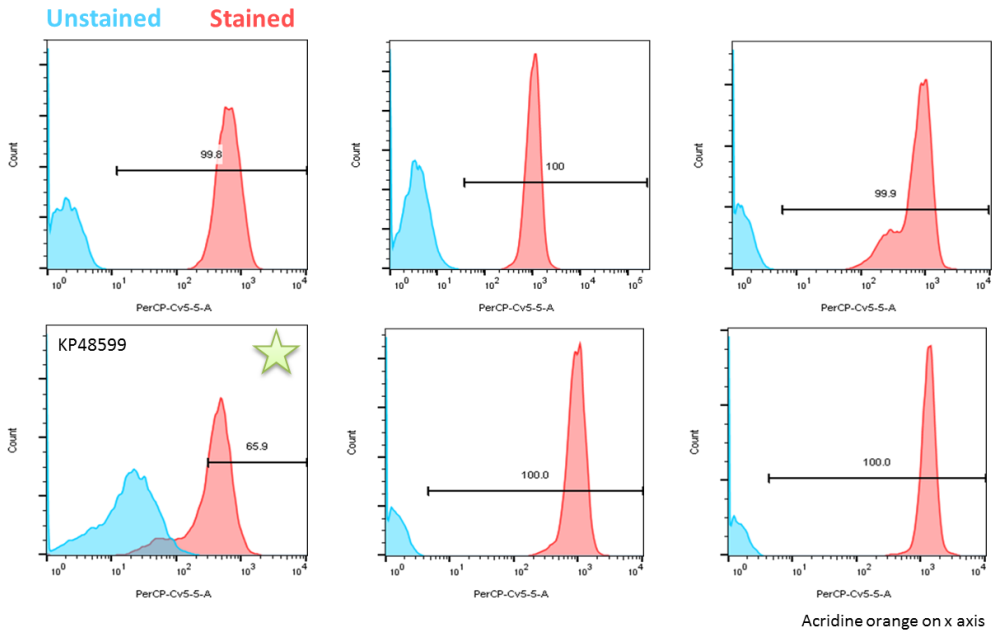

Figure 18 – The arbitrary drawing of gates in flow cytometry can be misleading.

The 65.9% result is a product of the unstained cell population having greater acridine orange fluorescence than the other samples (perhaps due to less efficient separation), as well as there being a left tail on the stained population that is not visible on the other samples. Additionally, since the gates are drawn arbitrarily from the left edge of the unstained histogram, there is considerable overlap between the two curves. Moreover, if the gate were redrawn to consider the behavior of the two curves an aberration (extend the curve more to the left), then the percentage of unique stained cells would change quite distinctly. The primary issue with that mode of analysis is the lack of statistical rigor to apply cutoff points and the arbitrary nature in which gates are drawn, particularly when there can be overlap between curves.

In an effort to apply statistics and compare more than just the unstained and stained $CD71^+$ populations, the acridine orange fluorescence in stained $CD71^+$ populations was compared to acridine orange fluorescence in the corresponding stained $CD71^-$ populations

(n=6). This accomplished two things: 1) it evaluated the separation efficiency of the CD71 immunomagnetic separation step and 2) it introduced another independent population for comparison with the $CD71^{+}$ stained cells. Point number two makes for a more interesting result because the data in the previous section just conveyed that the acridine orange was complexing with RNA in the $CD71^{+}$ cell population. With this analysis, a difference in acridine orange binding between the two populations on the basis of CD71 expression can be shown. When acridine orange fluorescence in $CD71^{+/-}$ cells stained with the dye were compared, a shift in the peak fluorescence between $CD71^{+/-}$ cells was evident and Figure 19 shows a representative plot of this shift between the two populations' distinct acridine orange fluorescence levels. Future analysis of $CD71^{high/low}$ expression as a function of RNA content is also possible to further stratify the $CD71^{+}$ cell population.

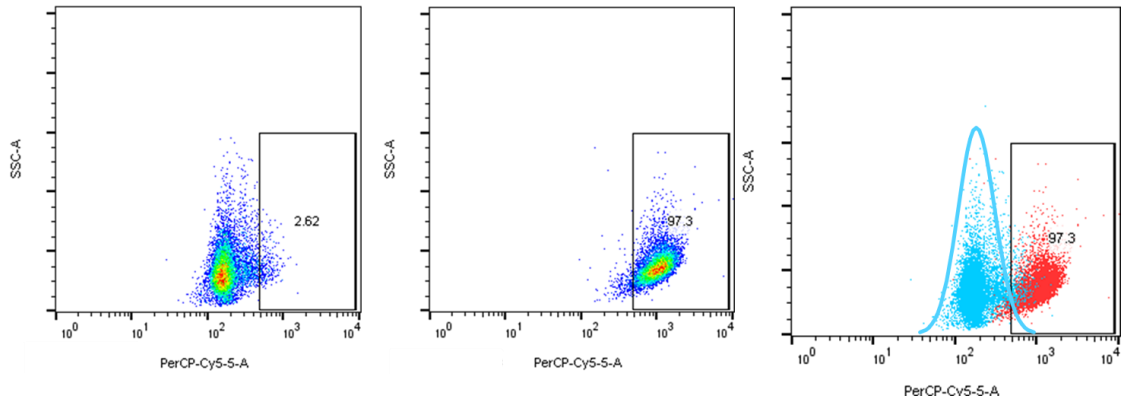

Figure 19 – Representative image comparing acridine orange fluorescence (x axis) in stained $CD71^{+/-}$ cells. Also a graphical one-tailed, 97.5% confidence level t-test.

Further statistical analysis was completed to determine the significance of the shift in mean acridine orange fluorescence shown in Figure 19. A 2.5% cutoff was imposed on the right tail of acridine orange fluorescence for the acridine orange-stained $CD71^{-}$ population to perform a 97.5% confidence level t-test on the difference between the mean acridine orange fluorescence for the $CD71^{+/-}$ populations. The mean acridine orange

fluorescence for six stained $CD71^+$ and $CD71^-$ samples was computed and a one-tailed, unequal variance independent t-test ran to compare the means ($p < .025$). These data indicate that the two populations were distinct based on their acridine orange fluorescence. In Figure 19, 97.3% of the $CD71^+$ cells fall within the 2.5% cutoff region, indicating an efficient separation of the $CD71^+$ cells from the corresponding $CD71^-$ cells from this donor. A hypothetical normal distribution curve is drawn on the $CD71^-$ curve to illustrate the t-test in action. Table 5 shows the mean acridine orange fluorescence for the stained $CD71^{+/-}$ populations from each donor. The fluorescence values are expressed in arbitrary units indicating the magnitude of the fluorescence. Notice that the aberrant sample from Figure 18 (KP48599) does not deviate as much from the other samples with these measures.

Table 5 – Mean acridine orange (AO) fluorescence for stained $CD71^{+/-}$ cells.

Sample	$CD71^-$ cell mean AO fluorescence	$CD71^+$ cell mean AO fluorescence	Cells in 2.5% cutoff region (%)
KP48474	235	652	76.5
KP48511	190	1016	97.3
KP48556	57.3	757	99.9
KP48599	62.4	408	85.2
KP48635	300	935	83.0
KP48660	362	1425	87.9
Mean	201.1	865.5	88.3
SEM	50.6	142.3	3.62
Effect size (Cohen's d)	2.54	p value ($\alpha = .025$)	0.0021

Stained $CD71^-$ cells had nearly four times less acridine orange fluorescence than the $CD71^+$ cells on average. The p-value returned by the one-tailed t-test and the effect

size measuring the distance between the population means as a fraction of the pooled standard deviation also indicate the significance of the difference between the two population means. An average of 88.3% ± 3.62% of the $CD71^+$ cells fell within the right 2.5% cutoff region of the $CD71^-$ population. Achieving close to 90% of the $CD71^+$ population being distinct from the corresponding $CD71^-$ population was quite remarkable. The R code used to perform all the F- (for homoscedasticity) and t-tests is shown in Figure 20. The lines are commented for clarity. Taken together, these data confirm the presence of RNA in $CD71^+$ cells.

```
neg <- c(235, 190, 57.3, 62.4, 300, 362) #AO fluorescence in CD71neg cells
pos <- c(652, 1016, 757, 408, 935, 1425) #AO fluorescence in CD71pos cells

#Test equality of variances using two-sided F test, alpha = .05
#null: ratio of variances = 1; alternative: ratio of variances ~=1
var.test(neg, pos);
#p-value = 0.04057, reject null so variances unequal

#Perform one tailed t-test, alpha = .025
#null: mu_pos - mu_neg = 0; alternative: mu_pos - mu_neg > 0
t.test(pos, neg, mu=0, alternative = "g", paired = FALSE, var.equal = FALSE, conf.level = .975)
#p-value = 0.002076, reject null
```

Figure 20 – R code to perform statistical tests.

3.3.4 Brilliant Cresyl Blue Detection of RNA in $CD71^+$ Cells

Brilliant cresyl blue staining of $CD71^{+/-}$ cells after CD71 immunomagnetic separation detected RNA granules in the $CD71^+$ cells (Figure 21). The cells, indicated by the black arrows, have a noticeable reticulum akin to Stage 3 in Figure 2. Cells in the corresponding $CD71^-$ cell samples did not contain these RNA granules (Figure 22).

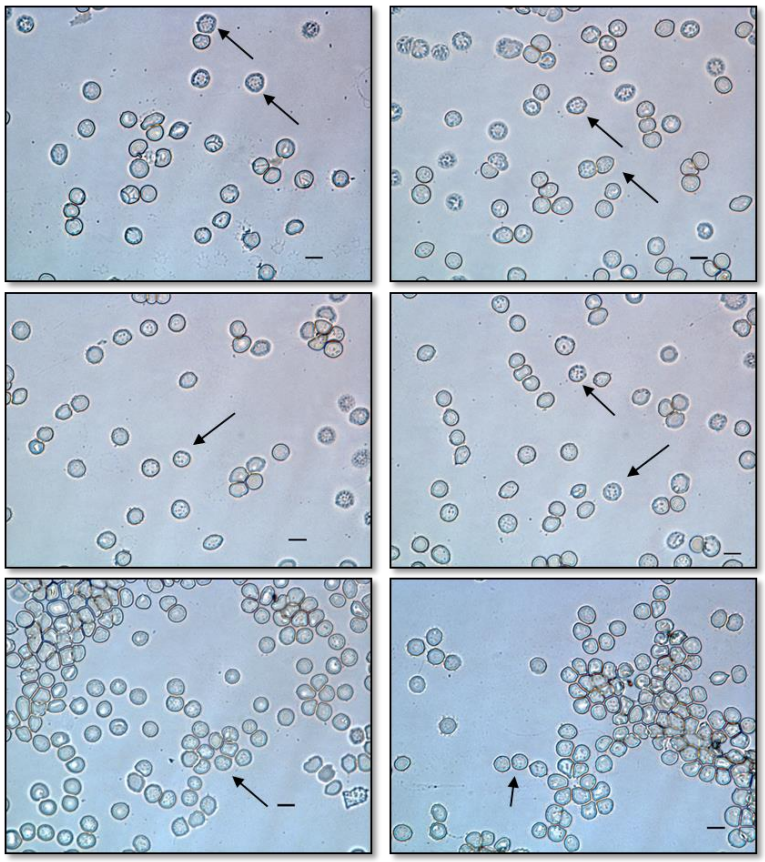

Figure 21 – Reticulated cells detected in CD71^{+} cell samples. Scale bar: 10µm.

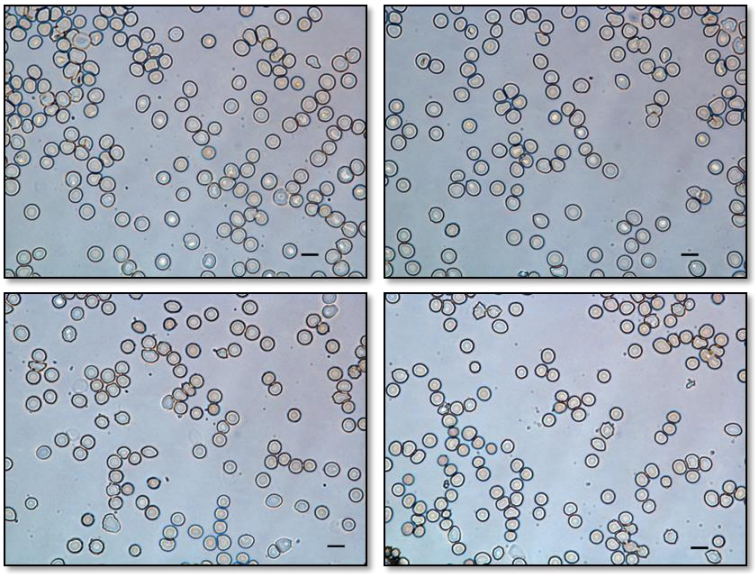

Figure 22 – Reticulated cells were not detected in the majority of the CD71^{-} cell samples. Scale bar: 10µm.

In a scan of the $CD71^-$ population slides, reticulated cells similar to the cell in Stage 4 of Figure 2 were detected (Figure 23). These cells likely accounted for the acridine orange fluorescence detected in stained $CD71^-$ cells (Figure 19). This result suggests that there may be a continuum of CD71 expression and RNA content along which reticulocyte maturation occurs. In this case, the $CD71^-$ cells still have detectable levels of RNA, but may not have a high enough level of CD71 to be detected. By one measure they can be classified as reticulocytes, but not by the other. There is also the possibility that the magnetic bead concentration used may not be high enough to capture all the $CD71^+$ cells in the post-Percoll separation sample. However, given the expense of the magnetic beads raising the concentration may not be feasible with the financials constraints of individual laboratories. Ultimately, immunomagnetic separation is not expected to result in complete isolation of all reticulocytes, presuming that the ones detected in Figure 23 still have some undetectable level of CD71. Moreover, the yield of nearly 90% distinct $CD71^+$ cells following immunomagnetic separation was an acceptable result for the purposes of this thesis.

Figure 23 – Reticulated cells detected in a $CD71^-$ cell sample. Scale bar: 10µm.

3.4 Aim 1 Summary

In this aim a detailed and visual method for the isolation of $CD71^+$ reticulcoytes from human peripheral blood was demonstrated. Rather than isolating from cord blood, which is not always available, the challenge of isolating these cells from what is considered a poor reticulocyte source (Moreno-Pérez, 2013) was undertaken. Through the combination of both density-dependent and immunomagnetic separation steps, an average of $2.47x10^6 \pm 7.49x10^5$ $CD71^+$ cells were isolated. While this yield is low relative to the trillions of cells in a 10mL whole blood sample, many assays can be performed with that quantity. Moreover, for disease samples in which steady-state peripheral reticulocyte levels can approach 10% of the total RBC count in the circulation like sickle cell disease (Lopez, 1996), higher yields would be expected.

Further study of the properties of the three bands observed after 70% Percoll separation is necessary to understand the functional differences that may exist between the layers, particularly as it relates to reticulocyte age and maturation. Extending these studies to disease samples (e.g., sickle cell, malaria, diabetes) would provide further insight into the specific densities or ages of reticulocytes that contribute (or do not) to specific pathologies.

Opportunities for innovation of the method also exist. Leukocyte and platelet depletion with the cellulose columns is the longest step in our method because of the dependence on gravity for the downward movement of the blood through the column. The introduction of an external pressure source or the engineering of a longer syringe barrel and plunger so that the sample and PBS washes can be passed through simultaneously

could reduce the time- and labor-intensiveness of the isolation procedure. The substitution of cellulose with a non-woven fabric filter may also reduce the duration of this step (Tao, 2011). The introduction of a solution would not only benefit this specific protocol, but more broadly fieldwork in which sample collection and processing cannot be done in traditional lab spaces.

For situations where there may be financial constraints around the expense of beads for immunomagnetic selection, the cells collected after 70% Percoll separation may also be sufficient for the experimental question being investigated (Russell, 2011; Noulin, 2014). Similarly, given the history of this laboratory, performing any of these steps with the throughput of a microfluidic device is also an intriguing thought.

CHAPTER 4. CD71$^+$ CELL RELEASE OF EXOSOMES IN VITRO

4.1 Introduction

Exosomes are vesicles generally 30-100nm in size that cells have been to found to release constitutively (Théry, 2002). First shown to be released by sheep reticulocytes *in vitro* (Pan, 1983) these nanometer-sized vesicles were thought to function in the developing red blood cell's removal of unneeded proteins and other intracellular components. Exosomes originate in multivesicular endosomes within cells that direct their components to the plasma membrane and eventually the extracellular space, rather than the cell's lysosomal pathway (Simons, 2009). Figure 24 shows the currently understood pathway for exosome biogenesis in mammalian cells.

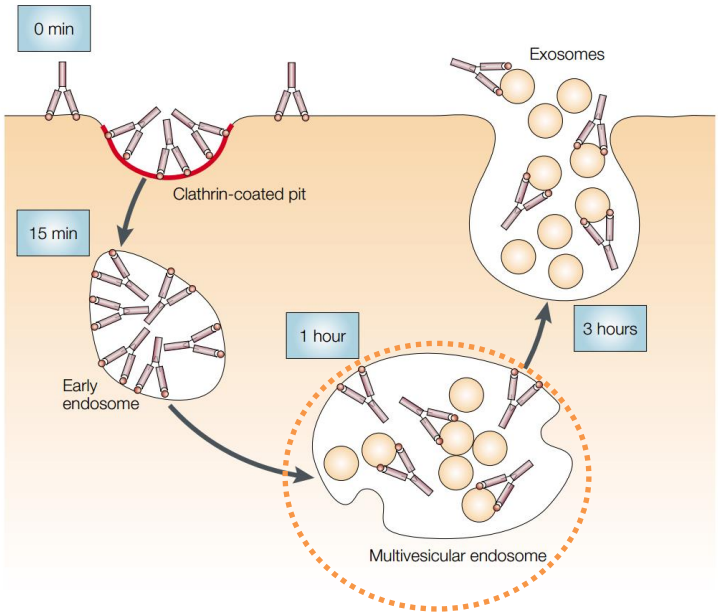

Figure 24 – Multivesicular endosome origin of exosomes (spheres). Adapted from Théry, 2002, page 570.

The macromolecule cargo (in this case, the transferrin receptor) is first packaged into endosomes. After some time, the receptor is complexed with individual exosomes in a larger multivesicular endosome. Once packaging is complete the exosomes are shuttled to and fuse with the plasma membrane and are then released into the extracellular space. Exosomes are generated within a cell through what is termed reverse intracellular-budding events Figure 25.

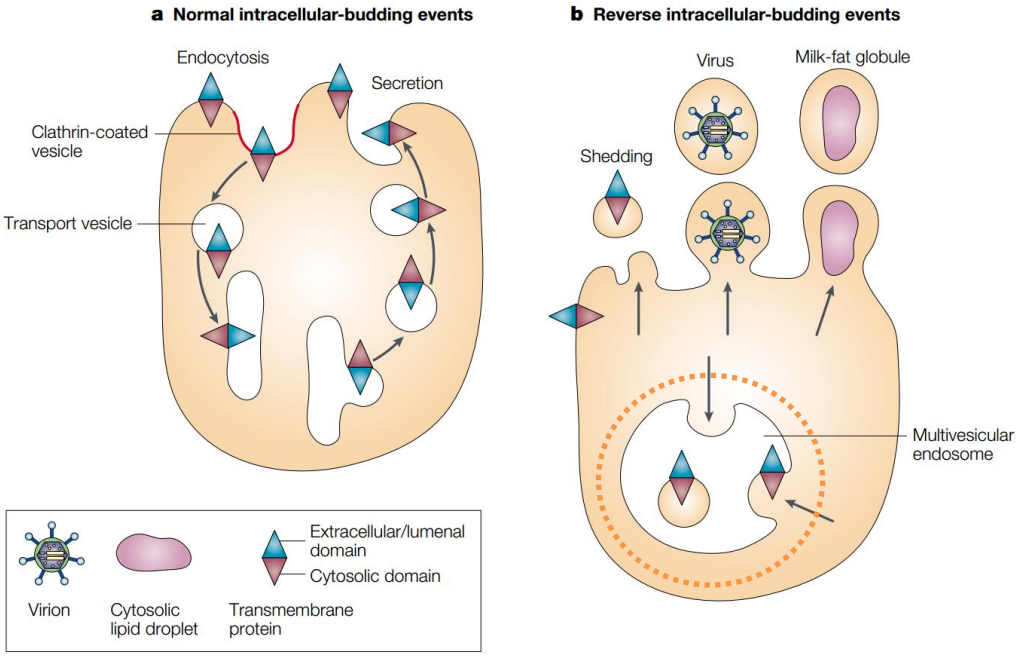

Figure 25 – Reverse budding of exosomes (on right). Adapted from Théry, 2002, page 570.

In a reverse budding event the cytosolic and extracellular orientation of the proteins in the cellular membrane is maintained in the exosomal membrane. In Figure 25 the extracellular domain (colored blue) of the protein is maintained on the outside of the exosomal membrane (facing the luminal compartment of the mutilvesicular endosome). When the exosome fuses with the plasma membrane and is exocytose the same orientation is maintained. Conversely, for normal intracellular-budding events, the cytosolic domain

(colored red) of the protein is moved to the outside of the transport vesicle. Current research is underway to determine more fully the mechanisms of exosome budding and secretion.

The reverse budding of exosomes intracellularly is important for their characterization with laboratory assays. Moreover, exosomes can be characterized not only by their size, but also by the expression of proteins that link them back to their endosomal origin. The expression of integrins and tetraspanins, heat shock proteins, and membrane transport proteins have been found to be relatively consistent across exosomes released by differing cell types (Théry, 2001; Théry, 2002; Simons, 2009). Tetraspanins are membrane-bound proteins and CD63 is highly enriched in exosomal populations (Simons, 2009). It is through the reverse budding intracellularly in which the presence of CD63 on a cell's membrane is maintained on an exosome's membrane.

Currently in sickle cell disease research much is known about red cell sickling, reticulocytosis, and red blood cell/reticulocyte adhesion to endothelial cells in the microvasculature (capillaries and post-capillary venules) (Rees, 2010; Barabino, 2010). However, there is still an overarching and critical need to develop therapies, which may require exploring new avenues. One area that has concentrated research efforts is the investigation of the factors the precipitate the onset of vaso-occlusion—the most common manifestation of the disease—in the microvasculature. The current understanding of vaso-occlusion is that reticulocytes initiate the process by adhering to the mature sickle red blood cells as well as white blood cells in circulation. Progressive blockage of blood flow follows (Barabino, 2010).

The clinical basis for this thesis takes what is known about cellular interactions in the sickle cell disease circulation and investigates the source of the pathology: the developing red blood cell, specifically the reticulocyte. Since the 1980s reticulocytes have been shown to exocytose intracellular materials during their development (Johnstone, 1987). By demonstrating the release of $CD71^+$ exosomes *in vitro*, this aim is a foundation for the study of the reticulocyte's intracellular processes (e.g., exosomal miRNAs and other macromolecule content) and the intercellular effects they can have in the reticulocyte's environment in the context of sickle cell. This provides the pathway for future investigation into the functional roles of exosomes and serves as a new direction in reticulocyte, and by application sickle cell, research. The availability of peripheral blood reticulocytes is especially tremendous for sickle studies because the procurement of cord blood reticulocytes is unlikely given the drawbacks to further segmenting the sickle patient population. Finally, recapitulating the finding of reticulocyte exosomes release *in vitro* by peripheral reticulocytes is a homage to original work done in sheep (Pan, 1983) and rats (Harding, 1983), and also reflects how long timelines in research can be.

To execute this aim exosomes were collected from the supernatant of $CD71^+$ reticulocytes incubated *in vitro* for twenty-four hours. Analysis of the exosomes by transmission electron microscopy, protein and RNA expression allowed greater characterization of the properties of these nanometer-sized vesicles and is a first step in further identifying their possible connection to pathologies.

4.2 Materials & Methods

4.2.1 Reticulocyte Culture Medium

CD71^{+} cells were incubated for 24 hours at 37°C in RPMI 1640 culture medium (Life Technologies) containing 10% v/v exosome-depleted FBS (Life Technologies), 2mM l-glutamine, 50 IU/ml penicillin (Corning/Mediatech), and 50ug/mL streptomycin (Corning/Mediatech). The exosome-depleted FBS purchased commercially was verified by the manufacturer to have removed 90% of the bovine cell-derived exosomes (Figure 26) and had no observable CD63 expression (Figure 27).

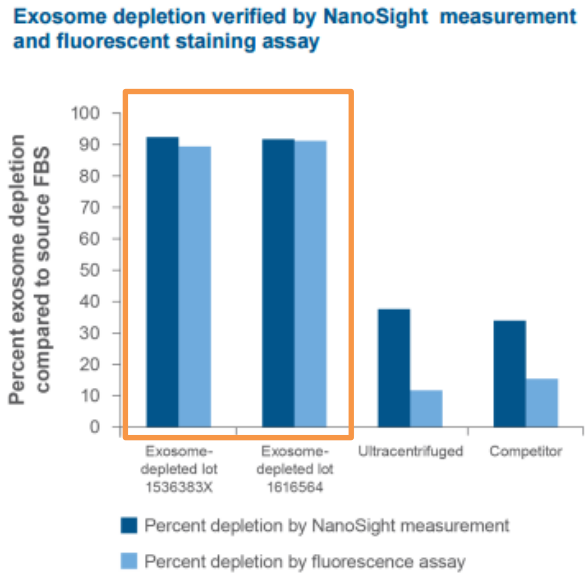

Figure 26 – 90% exosome depletion from FBS. Adapted from Paszkiet, 2016.

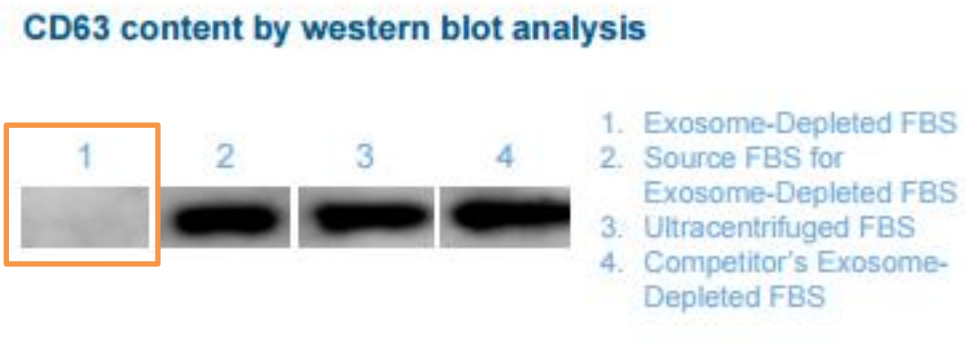

Figure 27 – No observable CD63 expression in exosome-depleted FBS (Panel 1). Adapted from Paszkiet, 2016.

4.2.2 Exosome Isolation

Exosomes were then isolated from the reticulocyte conditioned medium using ultracentrifugation (Théry, 2001). The cell culture supernatant was first centrifuged for 10 minutes at 2000g to remove any dead cells followed by centrifugation at 10,000g for 30 minutes to pellet cell debris. Exosomes were then pelleted during a 70 minute run at 100,000g. The exosome pellet was then resuspended in PBS to wash, and repelleted after another 70 minute 100,000g run. The exosome pellet was either resuspended in 100µL-200µL PBS for long-term storage at -80°C or prepared for a terminal assay. All centrifugation runs were performed at 4°C and speeds 10,000g or greater performed with the Beckman Coulter Optima™ MAX-XP Benchtop Ultracentrifuge, MLA-50 rotor, and OptiSeal polypropylene tubes. K562 cells, which are often used a cell line comparison in reticulocyte studies (Lozzio, 1975; Ttsiftsoglou, 1991; Bruchova-Votavova, 2010; Sangokoya, 2010), were cultured in the same medium and exosomes isolated from cultures of 10^7 cells.

4.2.3 Transmission Electron Microscopy

Exosome pellets were resuspended in 25µl 0.2M sodium cacodylate buffer (pH 7.4). 5µL of the sample was placed on Formvar 300 mesh copper grids (Ted Pella) and blot dried. 5µL 1% uranyl acetate was then delivered to the grid for a negative stain and blot dried. Samples were air dried prior to imaging at 30,000X-40,000X magnification on the JEOL- 2100 transmission electron microscope.

4.2.4 Total Protein Quantification of Exosomes

10µL of $CD71^+$ cell and K562-derived exosomes resuspended in 1X PBS were added to 40µL RIPA Buffer (ThermoFisher Scientific). 1X RIPA Buffer was prepared by supplementing 1mL RIPA with 10µL of the 100X Halt Phosphatase Inhibitor Cocktail (ThermoFisher Scientific), 10µL of the 100X Protease Inhibitor Cocktail (ThermoFisher Scientific), and 10µL of the 0.5M EDTA solution (ThermoFisher Scientific) to inhibit phosphatases, proteases, and metalloproteases, respectively. The exosome-RIPA protein homogenate was then sonicated three times for fifteen seconds at 37ºC. 400µL 1X PBS was then added to the solution and the supernatant collected after centrifugation for five minutes at 13000g and room temperature. The total protein concentration in the supernatant collected was then quantified with the microBCA assay (ThermoFisher Scientific) according to the manufacturer's instructions. The initial 1/45 dilution of the exosomal pellets was taken into account when calculating the total protein concentration in the samples.

4.2.5 CD63 ExoELISA

Exosomes were isolated from conditioned culture medium as described above. 5µg exosomal protein equivalent or 10µL of $CD71^+$ cell and K562-derived exosomes were used to perform the ExoELISA-Ultra CD63 kit (System BioSciences). The ELISA was completed according to the manufacturer's instructions. Measurements were read at 450nm on a spectrophotometer.

4.2.6 MiR-144 qPCR

Total RNA was isolated from K562 exosome and reticulocyte-enriched blood exosomes using Trizol LS (Life Technologies) according to the manufacturer's directions.

Total RNA was isolated from K562 cells using Trizol (Life Technologies) according to the manufacturer's directions. Trizol LS is better suited for liquid samples. Trizol homogenates for exosomal samples were loaded with 250fmol of the cel-miR-39 spike-in control (Qiagen). cel-miR-39 is regularly used as a spike-in control since no consensus exists for a housekeeping gene for miRNA expression in exosomes and because there is no homologous mammalian gene (Kroh, 2010; Kosaka, 2011; Roberts, 2014,). 5µL of a 15mg/mL solution of GlycoBlue coprecipitant (ThermoFisher Scientific) was added to the exosomal samples during the RNA precipitation step of total RNA isolation and the samples incubated overnight at 4ºC. Table 6 shows the target genes for the cellular and exosomal samples. For all samples mature miR-144 was targeted. For cellular samples, RNU6B, RNU48, RNU44, and hsa-miR-16 were used as housekeeping genes to normalize cellular miR-144 expression. These genes have been shown to be stably expressed in K562 cells (Applied Biosystems, 2010). Their C_T values were averaged and that average value used to normalize the cellular miR-144 expression for each sample. As described above, cel-miR-39 was used to normalize miR-144 expression in the exosomal samples.

500ng total RNA was reverse transcribed using the TaqMan MicroRNA Reverse Transcription Kit (Life Technologies) according to the manufacturer's instructions. After reverse transcription, the cDNA was amplified with the target primers in a standard 40-cycle quantitative polymerase chain reaction (qPCR) on the StepOne Plus (Applied Biosystems). Samples were run in triplicate. The thermal cycling conditions were as follows: 1) Hold for 10 minutes at 95ºC, 2) 40 Cycles of 15-second denaturing at 95ºC and annealing/extending for 60 seconds at 60ºC. TaqMan Universal PCR Master Mix (2X), no UNG (ThermoFisher Scientific) was used in the qPCR reaction mix. Also, the reverse

transcription and PCR primers for the genes in Table 6 were obtained from their respective TaqMan miRNA or gene expression assays. MiR-144 expression was quantified using the $\Delta\Delta C_T$ relative expression method, and the ΔC_T values are reported. ΔC_T was calculated as $C_{T,miR\text{-}144} - C_{T,housekeeping}$ for each sample. A positive value for ΔC_T indicated greater expression of the housekeeping gene than miR-144. Conversely, a negative value for ΔC_T indicated lesser expression of the housekeeping gene relative to miR-144. Mean C_T and ΔC_T values for each sample were reported with the standard error of the mean.

Table 6 – Target and housekeeping genes for cellular and exosomal samples.

Target gene	K562 cellular expression	K562 exosomal expression	Reticulocyte–enriched blood exosomal expression
miR-144-3p	X	X	X
Housekeeping genes			
RNU6B	X		
RNU48	X		
RNU44	X		
hsa-miR-16	X		
cel-miR-39 (spike-in)		X	X

4.2.7 Statistical Analysis

All population means are reported as the mean ± the standard error of the mean. To compare population means, one- or two-tailed (as indicated) Student's t-tests with 95% confidence levels ($\alpha = 0.05$) were performed. Prior to running the t-test a 95% confidence level F-test was used to test whether the variances of the populations were equal. The result

of that test is reported with the specific data. P-values less than 0.05 were considered indicative of a statistically significant result. Equation 1 on page 32 shows the formula used to calculate the effect size (Cohen's d) as another measure of the magnitude of the difference between two independent sample means. To account for differing sample sizes, a pooled standard deviation was used in the calculation of the effect size. The formula for the pooled standard deviation is in Equation 2 on page 32. All analyses were done in R or Excel. R codes are included in the appendix.

4.3 Results & Discussion

4.3.1 Transmission Electron Micrographs of Exosomes

Figure 28 shows TEM images of exosomes isolated from the culture medium of $CD71^+$ cells (top row, 40,000X) and K562s (bottom row, 30,000X) after twenty-four hours and with uranyl acetate counterstaining. The exosomes are the circles with distinct black outlines. The diameters of the exosomes pictured vary and fall into the expected 30-100nm size range (Théry, 2002).

A larger sized (~100nm) K562 cell-derived exosome was also imaged (Figure 29). This is similar to the large (~100nm) $CD71^+$cell-derived exosome in the first image on the top row of (Figure 28); it is indicated by a black arrow. These images are confirmation that exosomes are released by $CD71^+$ reticulocytes *in vitro*.

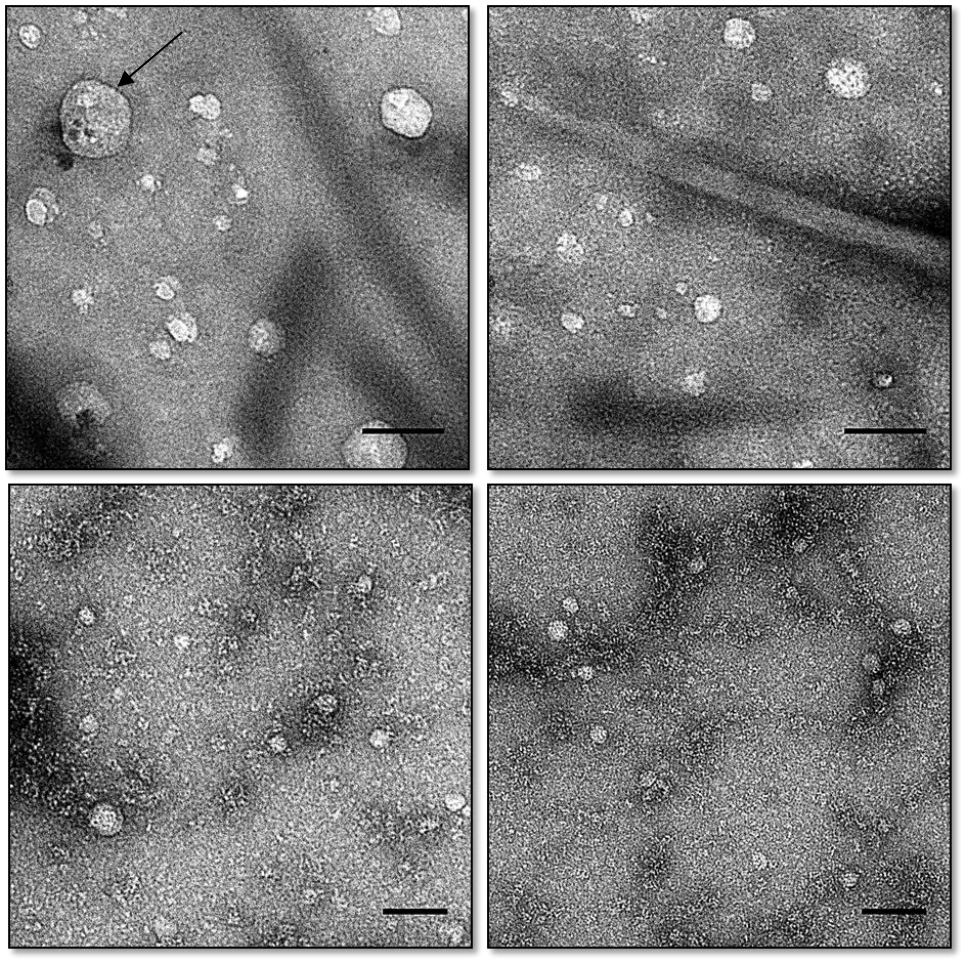

Figure 28 - TEM images of exosomes. Scale bars: 100nm.

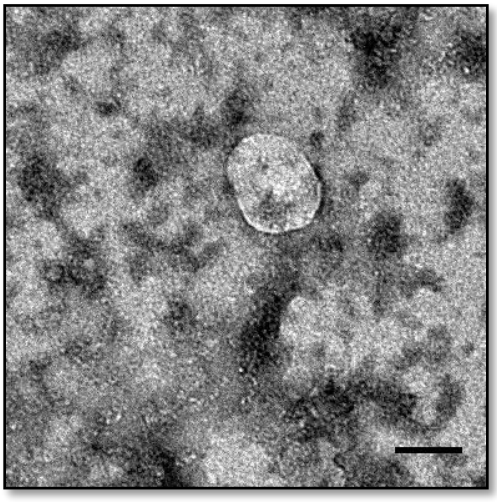

Figure 29 – Large K562 cell-derived exosome (30,000X). Scale bar: 100nm.

4.3.2 CD71$^+$ Reticulocyte-Derived Exosomes are CD63$^+$

The CD63 ExoELISA-Ultra was run according to the manufacturer's instructions to accomplish two tasks: 1) to quantify the number of exosomes in 5µg equivalent protein and 10µl samples of CD71$^+$ reticulocyte- and K562-derived exosomes and 2) to confirm that these exosomes are CD63$^+$, since CD63 is highly enriched on exosomal membranes (Simons, 2009). Figure 30 shows the standard curve derived from the ELISA data. Figure 31 shows the quantification of the number of CD63$^+$ exosomes in the 5µg equivalent protein samples. CD71$^+$ reticulocytes (n=3) released $35.8x10^9 \pm 22.8\ x10^9$ CD63$^+$ exosomes compared to $72.3x10^9 \pm 13.9\ x10^9$ CD63$^+$ exosomes released by K562 cells (n=5). When these two population means were compared with a two-tailed, equal variance, 95% confidence level student's t-test the difference between them was not significant ($p = .194 > 0.05$, effect size = 1.07). This suggests that the number of exosomes released by the two cell types was comparable, which was not an unexpected result.

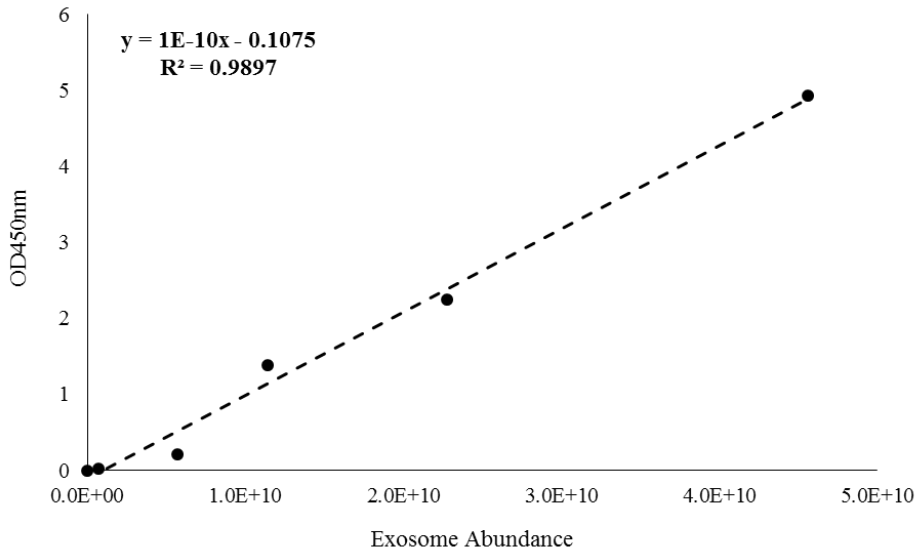

Figure 30 – CD63 ELISA Standard Curve. Optical density at 450nm on y-axis.

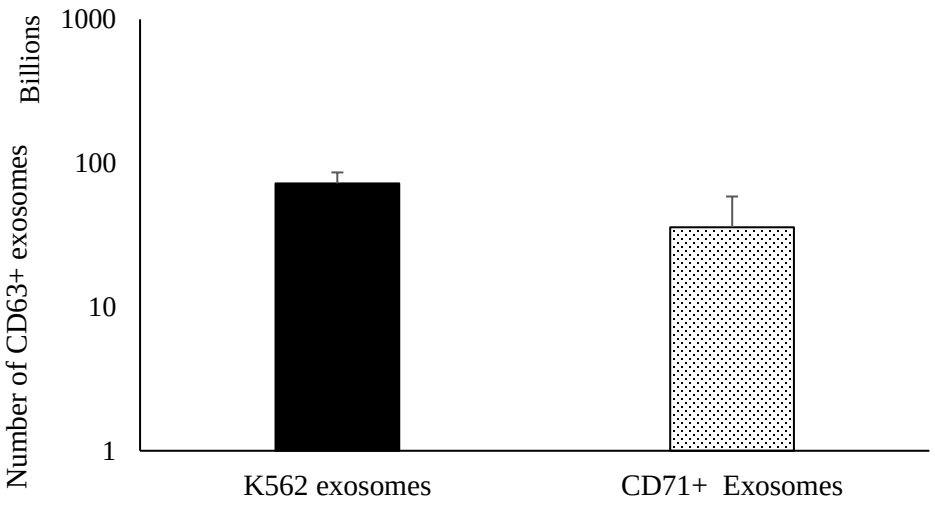

Figure 31 – 35.8x10^{9} CD63^{+} exosomes were released by CD71^{+} reticulocytes per 5ug equivalent protein (n=3); 72.3x10^{9} by K562 exosomes (n=5). The difference in exosome release was not significant (p > 0.05) suggesting the cell types released comparable amounts of exosomes even with differing starting cell numbers.

4.3.3 K562 Exosomal Protein Concentration is Greater

Figure 32 shows the total protein quantified in 10µl samples of CD71^{+} reticulocyte-derived exosomes and K562 cell-derived exosomes with the microBCA assay. The error bar for the CD71^{+} exosomes data point is too small to be seen on the y-axis scale.

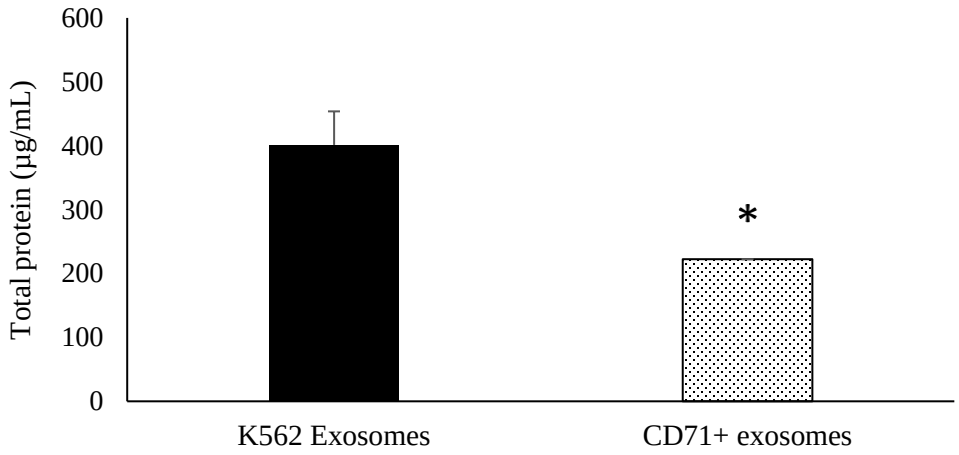

Figure 32 – K562 exosomes (n=5) package more protein than reticulocyte exosomes (n=3) (p < 0.05).

A one-tailed, equal variance, 95% confidence level t-test performed to compare the difference between the two mean protein concentrations found that the K562 exosomal protein concentration was significantly higher ($p = 0.044 < 0.05$, effect size = 1.86). These data suggest that at baseline the amount of protein in K562 exosomes is about twice that of the $CD71^+$ cell exosomes. However, further analysis was undertaken to determine whether this increased amount of protein was a factor of the total number of exosomes that was released by the cells instead of a factor of the amount of protein being packaged by the K562 cells into exosomes. This was undertaken because no significant difference, considering the standard error of the mean, was found between the total number of exosomes in the 5µg samples.

4.3.4 Exosome Release Potential

To determine whether the increased protein concentration in the K562 exosomes was a factor of total exosome release, the number of exosomes in 10µl samples of the two populations were determined at the same time the number of exosomes in the 5µg samples were determined. When the total protein concentration for each sample was divided by its corresponding number of samples Figure 33 was generated and protein content per exosome is shown. The data in Figure 33 suggest that the protein content/exosome is about five times greater in $CD71^+$ cells rather than the K562 exosomes. A two-tailed, unequal variance t-test comparing the two population means returned a p-value of 0.214 (effect size = 1.77). This data suggests that the protein content, when normalized to the number of exosomes, is comparable between the two exosome sources. This further corroborates the result in Figure 31.

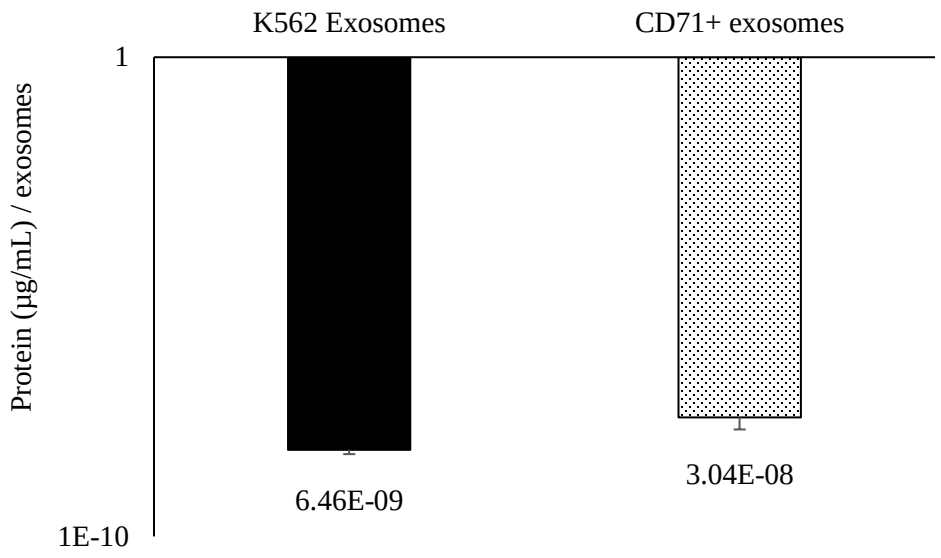

Figure 33 – Total protein concentration normalized to exosome release. K562 (n=5); CD71^{+} (n=3).

Similarly, the number of exosomes per microgram of protein in a millilitre of sample (for the equal 10µl aliquots) is comparable between the two populations, which is just an inversion of the data in Figure 33 (Figure 34, $p = 0.369$, effect size = 0.709). Figure 34 is also consistent with the data (speaking to the reliability in technique and performance of the ELISA kit) in Figure 31, where 5µg exosomal protein equivalent was used to determine the exosomal number in the samples. These figures were generated as a matter of appealing to individual preferences regarding normalization and data visualization. Both are not necessary for shorter reports. In actuality, Figure 31, Figure 32, and Figure 33 are quite sufficient.

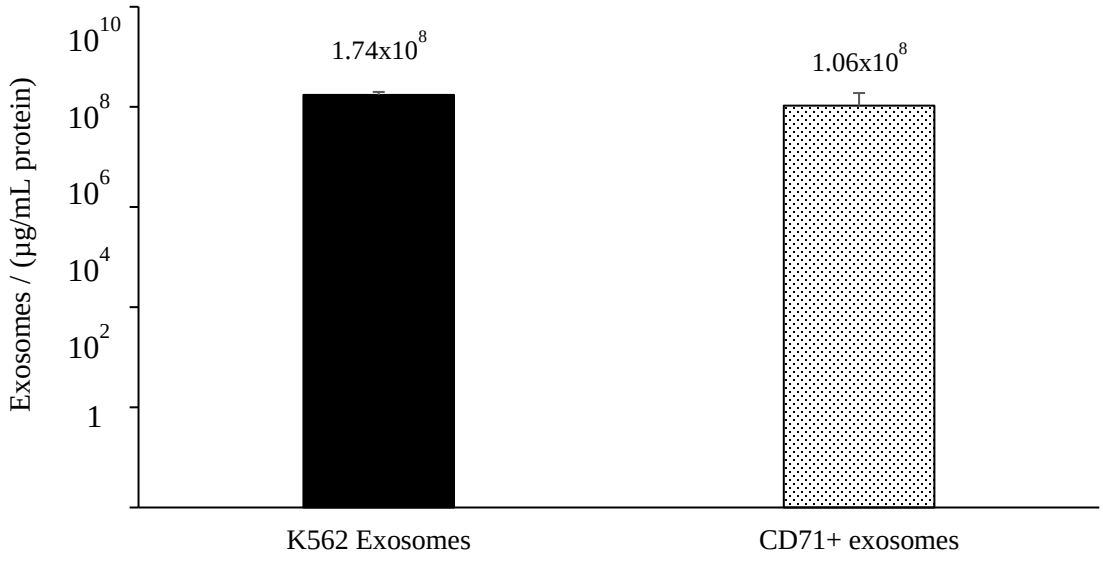

Figure 34 – Total exosome number normalized to protein concentraiton (10µL sample). Inversion of Figure 33. K562 (n=5); CD71$^+$ (n=3).

In what will be termed *exosome release potential* the more interesting conclusion that can be drawn from these data is that a fewer CD71$^+$ cells—for the three samples an average of $4.16x10^6$ cells—release a comparable (in absolute terms, 1.64 times less) number of exosomes as 10^7 K562 cells. Moreover, these exosomes package a similar amount of total protein. A lesser number of reticulocytes releasing this number of exosomes could speak to their maturing *in vitro* over the twenty-four-hour incubation period. This can be explained by the fact that exosome release by immortalized cell lines often requires stimulation or very high culture volumes and previously, K562s have had to be stimulated to release greater amounts of exosomes (Savina, 2003).

Taken together, these data lead to the following major conclusions. First, 10µl samples of K562 exosomes package more protein than the same volume of CD71$^+$ reticulocyte exosomes. Second, this increased protein packaging may be due to the greater number of K562s exosomes released, but once normalized there is no difference between

the two populations. It is worth noting that at the beginning of this analysis there were no expectations for the nature of the relationship between K562 and $CD71^+$ exosome release. The inclusion of K562 cells and exosomes in the study was for the purposes of having an independent group for comparison and to have a better sense of the scale of the results for the $CD71^+$ cells. These findings satisfy the reasoning for including the K562 cell line.

4.3.5 MiR-144 Expression in Healthy Exosomes Is Low

A preliminary qPCR analysis of the miR-144 expression was conducted in exosomes released into the culture medium of three reticulocyte-enriched blood samples incubated for twenty-four hours. Reticulocyte-enriched blood here means that CD71 immunomagnetic separation had not yet been implemented into the protocol. One of the reticulocyte-enriched blood-derived exosome samples was isolated from the culture medium of cells collected from Layer 1 of the three bands observed after Percoll separation. The other two exosomal samples was isolated from the culture medium of cells pooled from Layers 1 and 2 pooled. The reticulocyte-enriched blood-derived exosomal miR-144 expression was compared to both K562 cellular and miR-144 expression. Table 7 lists RNA concentrations for three reticulocyte-enriched blood samples and four K562 samples. The magnitude of the concentrations is similar for the two populations. Since this was a rough analysis no statistics were performed. MiR-144 expression was measured in the samples whose names in Table 7 are bolded. The miR-144 expression in the corresponding K562 cellular samples was also assayed. There was not enough total RNA (500ng) to run the qPCR with the samples not bolded.

Table 7 – Exosomal RNA concentrations.

Sample	RNA concentration (ng/µl)
KP45607 (L1 & L2)	22.06
KP45734 (L1 & L2)	48.11
KP45680 (L1)	44.07
9-Mar Flask 2	55.11
9-Mar Flask 3	18.04
10-Mar Flask 1	65.58
10-Mar Flask 2	34.62

The resultant C_T values, as well as the ΔC_T values after normalization to the housekeeping genes are shown in Table 8. Of the three K562 exosomal samples, only two had detectable miR-144 expression. The calculation of the standard error of the mean reflects this. The ΔC_T values are positive for both the exosomal and cellular samples which means that the housekeeping genes in all samples had higher expression levels than miR-144. MiR-144 expression was also higher in K562 cellular RNA than either exosomal sample. Since exosomes are nanonmeter-sized, it is no surprise that the RNA expression in the cell is greater. Follow-up analyses with $CD71^+$ reticulocyte cellular and exosomal RNA could provide more insight into the relative expression of miR-144 in a more purified cell population. However, the expression is expected to be low since blood donors are not anemic. MiR-144 is a marker of cell oxidative stress (Sangokoya, 2010) and is not expected to be elevated in healthy individuals' erythroid cells. Similarly, more analysis of RNA concentration and expression level by each 70% Percoll-separated layer could provide a deeper lens into the levels of RNAs as a function of reticulocyte age and maturation.

Table 8 – MiR-144 expression in cellular and exosomal samples. RB = reticulocyte-enriched blood.

	K562 cells (n=4)	K562 exosomes (n=3)	RB-derived exosomes (n=2)
miR-144 C_T Mean ± SEM	31.23 ± 0.87	37.23 ± 0.77	36.73 ± 0.02
ΔC_T Mean ± SEM	8.03 ± 0.81	13.33 ± 1.96	8.30 ± 0.57

4.4 Aim 2 Summary

In this aim, $CD71^+$ peripheral reticulocyte-derived exosomes were isolated from the culture medium of the cells after a twenty-four-hour incubation period. This is the first such demonstration of the isolation and collection of these exosomes from human peripheral reticulocytes *in vitro*. The exosomes were visualized with transmission electron microscopy and the validation of their expression of human CD63 then performed with ELISA. The total protein and RNA concentrations for these exosomes were also reported, comparing the levels to that of the K562 reticulocyte-like cell line. Overall, the nanometer-sized vesicles package small amounts of RNA and protein. However, the identification of specific RNAs and proteins warrants further investigation, particularly those with clinical relevance.

Further study is also needed on what was introduced as the exosome release potential of the $CD71^+$ reticulocytes. This could provide insights into the magnitude of exosome release during reticulocyte maturation. Additionally, evaluating the magnitude of exosome release for each of the three layers observed after 70% Percoll separation could provide a more granular view. One consideration is putting the magnitude of exosome release into

perspective. If in the circulation (which is the physiological context) there are many cell types *in addition to* reticulocytes releasing exosomes, then the following question arises: which cell type's exosomes has the predominant effect? One could speculate that the cell type with the highest absolute cell number may. However, the potency of a biological effect could be more dependent on the specific molecule and its biochemical action. Although the technical complexity would be increased, future experiments with multiple cell types may provide greater clarification on this issue. Overall, the intent is to uncover potential therapies and often, since biological molecules are studied in isolation, it can be difficult to sift through what are real physiologically-relevant effects and observations. Finally, extending these experiments to sickle cell disease samples could provide intriguing data on the exosomal profiles of sickle reticulocytes from the many angles described above. The possibilities are many.

On a technical note, the ELISA used to assay CD63 was prone to discrepancies and returned a high standard deviation for some of the standards, a result that has been noticed with products from the manufacturer (Franquesa, 2014). The high standard deviation could be due to the number of washing steps during the course of the assay, the potential to not completely remove unbound the primary or secondary antibodies, or to the possible mixing that can occur between wells during liquid removal. Currently, there are two primary techniques available to quantify exosomes: the Nanosight and the ExoELISA (System Biosciences). The ExoELISA is the much cheaper and less quantitative option (the exosomes used to build the standard curve are not reticulocyte- or K562-derived so CD63 expression is relative), but as alluded to earlier can be difficult to work with and may have quality control issues. The data that were presented here were the first successful runs after

testing three different ELISA kits prior. The previous kits were not the ExoELISA-Ultra and went off-market for some time. The primary challenge with the kits was the instability of the standards, which rendered quantitation of the exosomal samples impossible. Moreover, it appears that the ExoELISA-Ultra is a more reliable iteration of the product. More broadly speaking, more consistent quantification methods are needed, especially if access to the more robust NanoSight system is not available and given the expense of the ELISA.

CHAPTER 5. DELIVERY OF EXOSOMES TO ENDOTHELIAL CELLS

5.1 Introduction

The fate of exosomes once they are released into the extracellular space is the current interest of many investigators worldwide because of their potential to act as intercellular communicators via their packaging of RNAs and proteins. This idea of exosomes functioning as vessels for intercellular communicators has been reported with proteins, lipids, mRNAs, and miRNAs as the material exchanged between donor and recipient cells (Théry, 2002; Valadi, 2007; Simons, 2009; Kosaka, 2010; Iguchi, 2010). Moreover, this phenomenon has been reported to occur between monocytic THP-1 (donors) and human mammary epithelial cells (recipients) (Zhang, 2010). Whether a similar process occurs during healthy (or sickle) reticulocyte maturation between reticulocytes and other cells in the periphery is unknown. Figure 35 shows the many pathways of exosome delivery of macromolecules currently under investigation.

Much research on endothelial cells in sickle cell disease (SCD) has focused on cell adhesion to the endothelium that can promote vaso-occlusion. Extensive literature is available about the cytokines like TNF-α or IL-1β and integrins that play a role in both white and red blood cell adhesion to the vascular endothelium in SCD (Barabino, 2010). This aim introduces a new paradigm, reticulocyte-derived exosomes, of intercellular communication in erythropoiesis and possibly the promotion of SCD pathology. The results of this aim have implications not only for the understanding of the molecular

processes related to reticulocyte maturation, but overall endothelial cell function in healthy and potentially disease states. Ultimately, since sickle cell disease therapies are the goal, this aim opens the possibility for therapies directed not just at the mature RBC, but also the reticulocyte or endothelial cell.

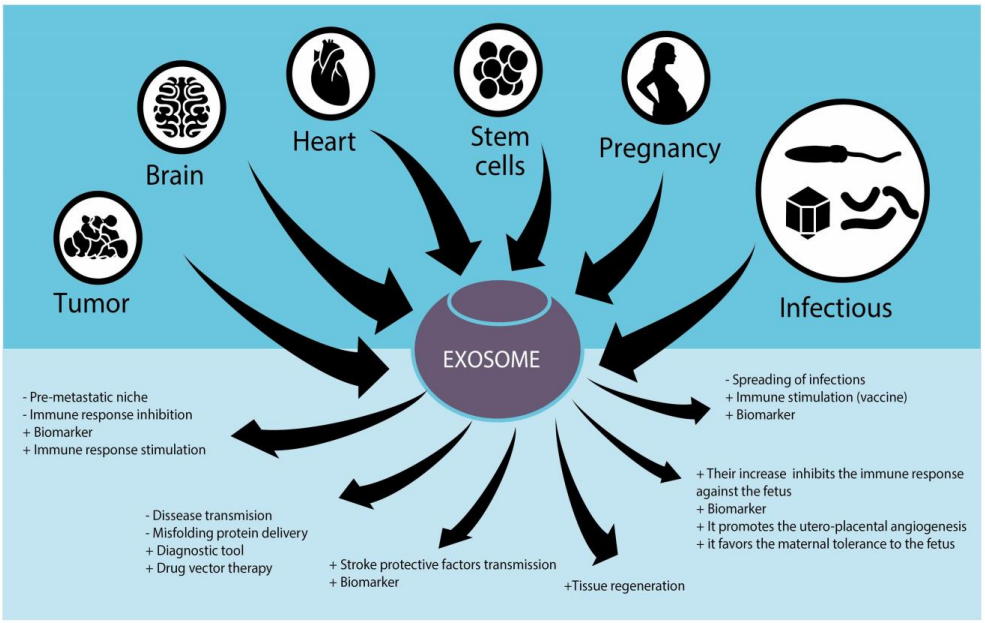

Figure 35 – Exosomes in human health. Adapted from De Toro, 2015, page 8.

5.1.1 An Aside on a Novel Mechanism in SCD

A part of the overarching clinical direction of the thesis was the possibility of miRNA exchange between peripheral reticulocytes and endothelial cells in both healthy and disease states. To build upon this because it is most relevant in this chapter and for comprehensiveness, the thinking and what formed the conception for this aim was that endothelial cells use reticulocyte-derived miR-144 (that was delivered via exosomes) as an external signaling cue for modulation of nuclear factor erythroid 2-related factor 2 (NRF-2) activity, a process that drives the endothelial cells towards a pro-inflammatory, pro-

adhesive, and more permeable state. The postulation is that reticulocyte promotion of vascular dysfunction in sickle cell disease is mediated by miR-144, an erythroid-specific miRNA discussed in Section 2.5. Reticulocyte miR-144 levels are elevated in sickle patients and are associated with anemia severity (Sangokoya, 2010). In sickle reticulocytes miR-144 has been reported to be a direct regulator of NRF-2, a transcription factor that controls the expression of a set of antioxidant related proteins (Sangokoya, 2010; Cheng, 2013). Moreover, increased levels of miR-144 in sickle reticulocytes are associated with decreased levels of NRF-2.

NRF-2 has been shown to mitigate the effects of the inflammatory cytokines tumor necrosis factor-alpha (TNF-α) and interleukin-1-beta (IL-1β) in endothelial cells, supporting its role as an anti-inflammatory agent (Chen, 2006). In sickle cell disease, TNF-α and IL-1β promote the expression of vascular adhesion receptors like vascular cell adhesion molecule-1 (VCAM-1) on the endothelial cell surface. These two cytokines also promote the production of interleukin-8 (IL-8), a chemokine secreted by endothelial cells that promotes reticulocyte adhesion to endothelial cells by activating and increasing the avidity of the α4β1 integrin on reticulocyte membranes (Belcher; 2000; Makis, 2000).

Therefore, downregulation of NRF-2 could promote increased TNF-α and IL-1β levels, directing endothelial cells to a more pro-adhesive state with the increased expression of adhesion receptors. TNF-α-induced secretion of IL-8 could also promote the pro-adhesive state. Finally, miR-144 reduction of NRF-2's anti-inflammatory effects in endothelial cells may lead to increased levels of vascular endothelial cell growth factor (VEGF) in endothelial cells as a pro-survival response. Increased VEGF levels could then

promote greater vascular permeability, which is one of VEGF's functions. The molecular process is shown graphically in Figure 36.

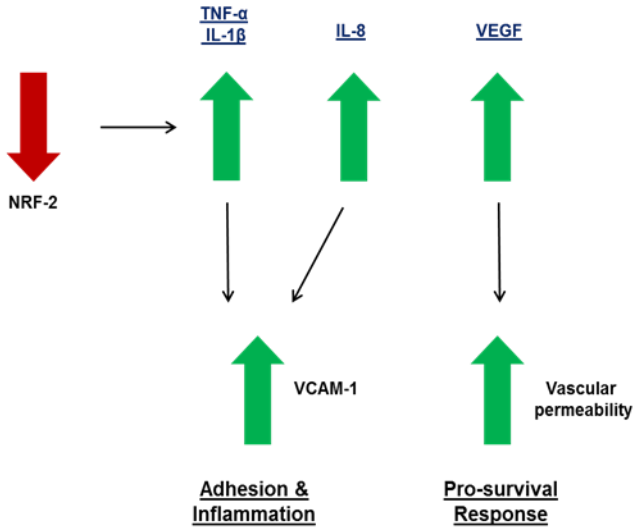

Figure 36 – MiR-144's effects on endothelial cells.

This aim establishes the experiments that will form the basis for future study of the mechanism described above by demonstrating that $CD71^+$ peripheral reticulocyte-derived exosomes are internalized by endothelial cells *in vitro*.

5.1.2 Experimental Design Considerations

To execute the aim, three parameters of the experimental design were first considered: 1) the cell source's exosome release per µg total exosomal protein, 2) the number of recipient endothelial cells, and 3) the geometry of the culture ware. The data in Chapter 4 shows that on an absolute basis the mean number of exosomes released by $CD71^+$ cells per five micrograms total protein is roughly half that of K562 exosomes. Therefore, the actual number of exosomes delivered to the endothelial cells would differ based on the apparent nonlinear relationship between exosome protein concentration and

exosome number. Oftentimes, published articles do not report both the protein equivalent and the exosomal number that is delivered so different approaches were taken with the K562 exosomes (since the supply is more easily replenished), followed by the $CD71^+$ exosomes as described in the Materials & Methods section. The number of recipient endothelial cells was also considered a tunable parameter because too many cells could diffuse the fluorescent signal indicating internalization of the exosomes. Finally, related to the number of endothelial cells was the geometry of the culture ware upon which the cells would be seeded. Since endothelial cells are adherent, considering their recommended seeding density (in this case, 2500 cells/cm^2) was needed to determine the correct geometry that would not preclude the previous parameter of total recipient cell number.

5.2 Materials & Methods

5.2.1 Endothelial Cell Culture

Human umbilical vein endothelial cells (HUVECs) purchased from Lonza were cultured up to passage 5. The cells were cultured in endothelial cell basal medium (EBM-2; Lonza) supplemented with the components in the EGM-2 BulletKit (Lonza): human epidermal growth factor, 0.5mL; vascular endothelial growth factor, 0.5mL; R3-insulin-like growth factor-1, 0.5mL; ascorbic acid, 0.5 mL hydrocortisone, 0.2mL; human fibroblast growth factor-beta, 2mL; heparin, 0.5mL; fetal bovine serum, 10 mL; gentamicin/amphotericin-B, 0.5mL. No adjustments to the media formulation were made. The cells were seeded at a concentration of 2500 cells/cm^2 on flasks coated with 1% gelatin (Sigma) and incubated at 37°C and 5% CO_2.

5.2.2 Fluorescence Staining of Exosomes

On the day prior to exosome incubation, 5000 HUVECs were seeded onto a 35mm dish with a No. 1.5 10mm glass insert coated with 1% gelatin (Mattek). The culture medium volume was initially brought to 1mL to allow the cells to settle after seeding. After one hour, the total volume in the dish was brought to 2.5mL. On the next day, the cells were incubated with exosomes.

5.2.3 Exosome Incubation with Endothelial Cells

Each exosomal sample was stained with BODIPY TR ceramide (ThermoFisher Scientific). The dye was purchased as 250µg of lyophilized powder. It was reconstituted in 354.25µL DMSO to prepare a 1mM stock upon receipt, aliquoted, and stored at -20°C prior to use. 1µL of the stock dye solution was delivered to 100µg or 20µg protein equivalent of K562 exosomes or approximately 20µg protein equivalent $CD71^+$ exosomes. The protein equivalent for the $CD71^+$ exosomes varied, as entire samples were used to maximize the total number of exosomes delivered to the endothelial cells. The total volume of the exosome plus dye solution was brought to 100µL with 1X PBS. The exosomes were stained for 20 minutes at 37°C in the dark. Control samples (1X PBS) were also treated with the same concentration of dye for the same amount of time. After the incubation, the exosome solution was filtered through exosome spin columns (Life Technologies) according to the manufacturer's directions to remove unbound dye. The stained exosomes were then incubated with the HUVECs in the 35mm glass-bottom dishes with 10mm glass inserts for two hours at 37°C. After the two-hour incubation, the HUVECs were washed with warm 1X PBS and fixed with 10% neutral-buffered formalin (Fisher) for fifteen

minutes at room temperature. After fixation the cells were washed three times with 1X PBS, mounted with DAPI-Fluoromount-G (Southern Biotech), and a coverslip put atop the glass insert. The cells were imaged on the Nikon Eclipse T_i inverted fluorescence microscope at 20X magnification, 19ms exposure on the DAPI (blue) channel and 300ms exposure on the DSRED (BODIPY TR Ceramide) channel. Figure 37 shows the experimental approach graphically. No look-up tables were used to scale or augment the red fluorescence in the images.

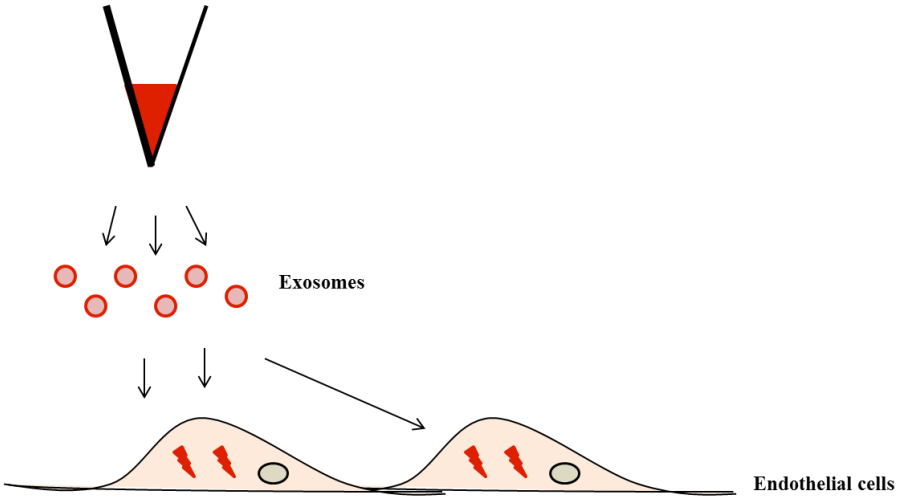

Figure 37 – Aim 3 Experimental Approach. Exosomes are labeled with dye that fluoresces red. Endothelial cells that internalize stained exosomes are expected to fluoresce red.

5.3 Results & Discussion

Figure 38 and Figure 39 show the fluorescence detected in HUVECs treated with 100µg protein equivalent of K562 exosomes after two hours. The cell nuclei are stained blue with DAPI. The exosomes, particularly in the concentrated areas where there are dots, appear to localize along the periphery of the cell nucleus and throughout the cytoplasm. BODIPY TR ceramide is a sphingolipid analog that has traditionally been used in Golgi

apparatus trafficking and tracking studies. So, it is possible that exosomal membranes, which is where the dye would have localized during staining, fused with nuclear and organelle membranes within the endothelial cells. No fluorescence was detected in the cells that were treated with the 1X PBS control (Figure 40). These data indicate that endothelial cells internalize K562 cell-derived exosomes and imply the possibility that intercellular communication via exosomes could occur between the two cell types.

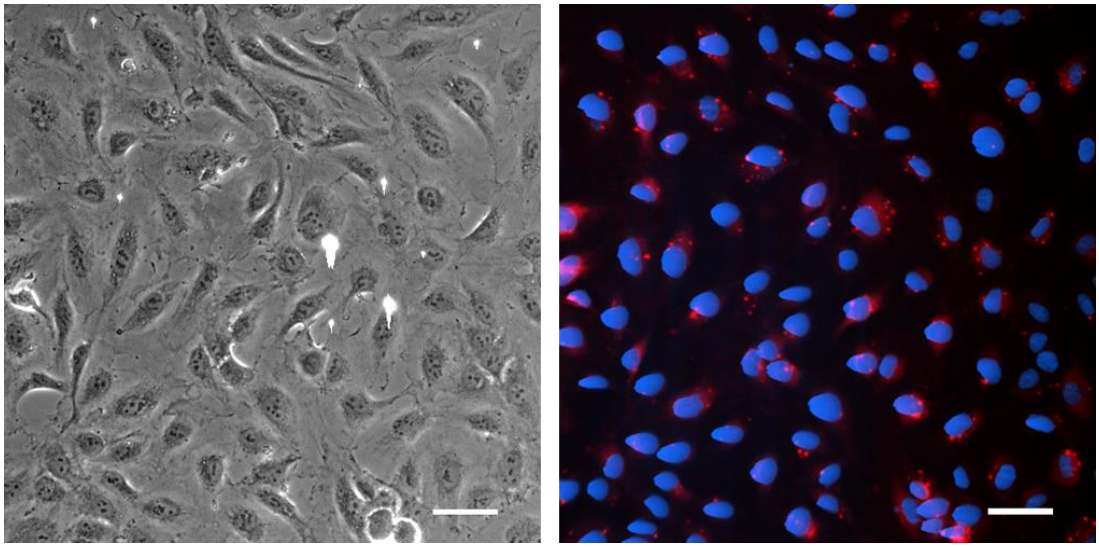

Figure 38 – HUVECs incubated with 100µg exosomes (red) for two hours. Scale bars: 50µm.

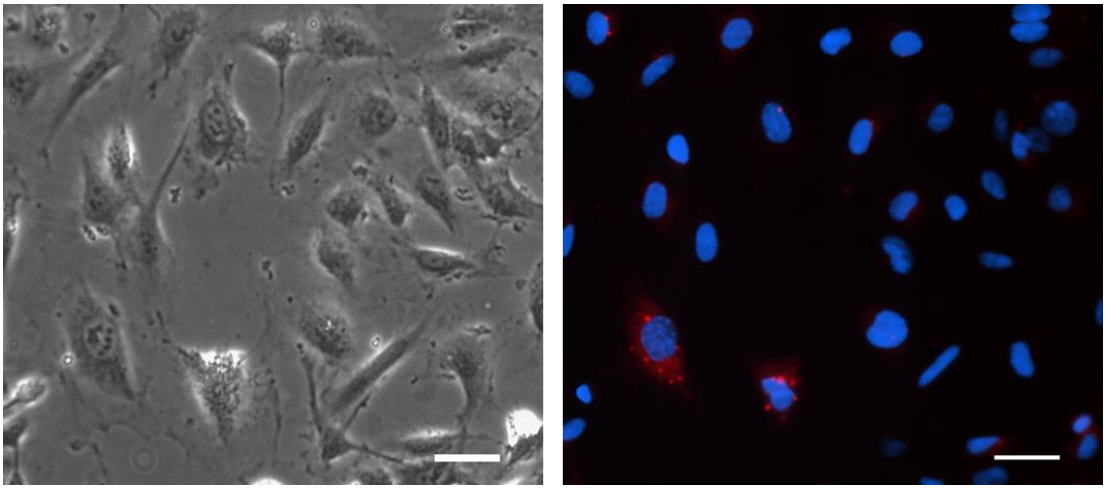

Figure 39 – HUVECs incubated with 100µg K562 exosomes (red). Scale bars: 50µm.

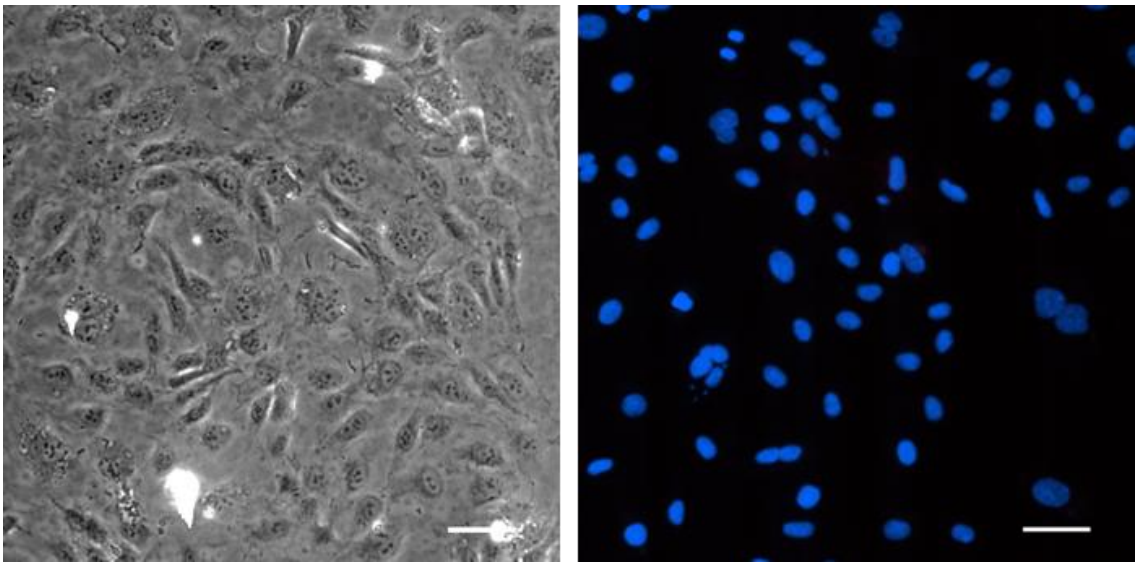

Figure 40 – HUVECs incubated with PBS + dye (red) for two hours. Scale bars: 50µm.

The observation was made that the results for the data above reflected nearly five time the amount of the total $CD71^+$ exosomal protein amount (~20µg). Therefore, to determine what fluorescence signal ~20µg protein equivalent of K562 exosomes would result in, that amount of exosomes was also delivered to HUVECs, the results of which are shown in Figure 41. DAPI-stained nuclei were not layered onto the images of the BODIPY ceramide fluorescence because of the greater intensity of the DAPI fluorescence. The BODIPY ceramide fluorescence was captured with the same exposure time (300ms). The difference in fluorescence intensity is readily noticeable. PBS control results are shown on the third panel. Given that the $CD71^+$ cells release on average two times less exosomes, the decision was made to pool the $CD71^+$ exosome samples because there appears to be an exosomal number below which fluorescence after staining with BODIPY cannot be detected. No internalization was detected as summarized in Table 9, which suggests uptake may be recipient cell type-dependent.

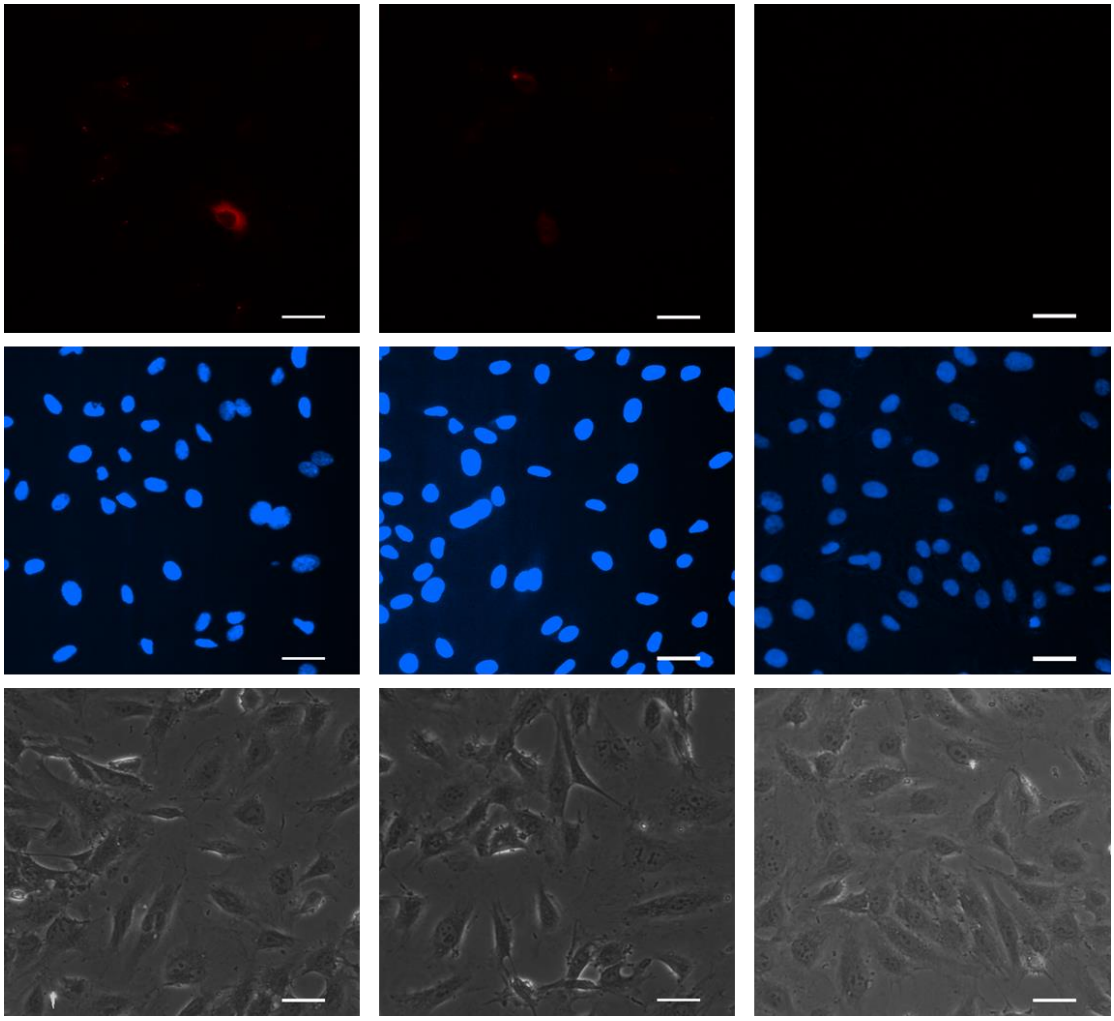

Figure 41 – HUVECs incubated with 20µg K562 fluorescent exosomes (red) for two hours in the first two panels. Scale bars: 50µm.

Table 9 – Summary of reticulocyte exosome-HUVEC studies.

Experiment	Exosome protein equivalent	No. endothelial cells	Fluorescence?
1	20 µg	5000	No
2	20 µg	2500	No
3	60 µg	2500	No

5.4 Aim 3 Summary

In this aim K562 cell exosomes were delivered to endothelial cells and allowed to incubate for two hours. Imaging demonstrated that the exosomes were internalized by the endothelial cells. Inspection of the fluorescence images indicated that the exosomes localized outside of the cell nuclei and throughout cytoplasm, suggesting fusion with the cell's endomembrane system. HUVEC incubation with $CD71^{+}$ reticulocyte-derived exosomes resulted in no detection of internalization, suggesting cell-specific internalization of the exosomes. Since reticulocytes are hypothesized to interact with vascular endothelial cells, future studies using human microvascular endothelial cells or human aortic endothelial cells may be more appropriate. However, the tissue-specific internalization of the exosomes may be a barrier—i.e., most commercially available human microvascular endothelial cells are derived from dermal tissues so the exosomes may not be internalized by those cells either.

Further study on where the exosomes are localizing is a viable future direction, and could be completed with the concomitant staining for organelles markers, e.g., Golgi, endoplasmic reticulum, etc. Similarly, more time points could provide more insight to trafficking of the exosomes within the endothelial cells as a function of time and location. Additionally, RNA- or protein-specific dyes could be used to determine where these macromolecules are being delivered holistically within the endothelial cells. The caveat there would be that because exosomes package so little RNA and protein, visualizing this localization may require large amounts of sample.

Beyond studies on exosome localization, determining the functional effects of the exosomes after specific times is of interest, particularly in disease states. For sickle cell disease, the mechanism described in this chapter's introduction is the obvious next step of analysis once sickle samples can be procured. Technically, once the samples are acquired execution should be fairly straightforward because the required techniques (reticulocyte isolation, cell culture, exosome isolation, protein quantification, etc.) are now standard. Unmasking the nature of reticulocyte exosome "communication" with endothelial cells would open a new paradigm in sickle cell research, and reticulocyte biology in general. Finally, given the history of the laboratory in which this thesis was conducted, performing these experiments under dynamic flow in microfluidic devices rather than static conditions would add another physiologically relevant parameter to the *in vitro* experiments. Since red cells are in constant motion in the circulation, performing exosome incubation studies under flow could be a better model for their native environment. Using microfluidic devices to recapitulate processes in the vasculature is one of the main advantages of designing these devices (van der Meer, 2009).

CHAPTER 6. CONCLUSION

The ability to isolate reticulocytes from peripheral blood offers the opportunity to better understand this cell type's function in healthy and disease states. As an extension, uncovering the role of reticulocyte-derived exosomes in disorders where reticulocytes may be a source of pathology is critical to more fully understanding the progression and steady states of those diseases. The method for the isolation of human peripheral reticulocytes detailed visually in Chapter 3 is straightforward and requires standard lab equipment except for the immunomagnetic separator, features that can lead to its wide adoption. Moreover, to this group's knowledge it is the first demonstration of human peripheral $CD71^+$ reticulocyte isolation at such a thorough level and without the partitioning of samples, which was not previously available in the literature. The primary work from which this thesis was adapted was a cord blood reticulocyte enrichment method and its relatively recent publication date (2011) indicates the limited methods available for reticulocyte isolation from either peripheral or cord blood. Furthermore, this thesis making peripheral blood reticulocytes available for *in vitro* use is especially tremendous for future sickle cell disease studies because the procurement of cord blood reticulocytes is unlikely given the sample size drawbacks to further segmenting the sickle patient population by gender and pregnancy status. The observation of three distinct bands above the 70% Percoll cushion, which has not been reported previously, offers the opportunity to study each layer individually and extrapolate the findings to insights about reticulocyte age and maturation. Moreover, after CD71 immunomagnetic selection approximately 90% of the $CD71^+$ population being distinct from the corresponding $CD71^-$ population per sample when

measured via flow cytometry was achieved, showing the success of this thesis' isolation procedure. In addition, the further isolation and characterization of human peripheral $CD71^+$ reticulocyte-derived exosomes in this study are the first demonstration of these phenomena with a pure population of human peripheral cells and are the foundational studies needed for the more mechanistic investigations on reticulocyte maturation and exosome function that will likely follow this thesis.

The technical limitations of the work, when applicable, are detailed in each specific chapter. However, the overarching limitation to the breadth of this work was the absence of sickle cell patient samples, the procuring of which can be especially difficult due to limited patient access and the establishing of connections with hospitals. However, great care was taken to emphasize the clinical relevance of this thesis to sickle cell disease because the pathology formed the conceptual basis for the aims that were performed. Additionally, all the blood donors in this thesis were African-American because the expectation is that should sickle samples be acquired in the future, these data will be used as the control samples.

The development of a method for the isolation of reticulocytes from peripheral blood undoubtedly provides opportunities for the conducting of studies that could not once be done due to the limited availability of these cells. From erythropoiesis to specific disease states in which reticulocytes drive pathology, the opportunities are many for the use of human peripheral reticulocytes in future investigations. Table 10 lists future research directions by specific aim. Due to the research thrust in the laboratory in which this thesis was performed being sickle cell disease, an emphasis on sickle cell is made in these future directions.

Table 10 – Future research directions.

Aim	Topic (emphasis on SCD)
1	Innovation with protocol (discussed in Chapter 3)
1	Use of isolation methods with disease samples
2	Time course studies of exosome release by $CD71^+$ cells *in vitro*
2	Healthy/sickle exosomal transcriptome and proteome profile
2	$CD34^+$ cell differentiation and exosome retrieval (reticulocyte exit)
3	Response of endothelial cells to reticulocyte-derived exosomes (healthy/not healthy)
3	Sickle exosome binding via the $\alpha_4\beta_1$ integrin to endothelial cells
3	Microfluidic device studies with exosome-treated endothelial cells

As discussed in Chapter 3, the peripheral reticulocyte isolation method introduced is not fixed and is open to innovation, particularly at the leukocyte and platelet depletion step. The extension of the syringe barrel to load the entire sample and PBS washes could reduce the length of the protocol by at least two to three hours. The shortening of that one step could reduce the labor- and time-intensiveness of the technique considerably. Extending the method to disease samples, like sickle cell disease which has been mentioned, as well as malaria or diabetes could prove it to be a useful source of peripheral reticulocytes—especially since currently it is not considered so (Moreno-Pérez, 2013).

As discussed in Chapter 4, time-course studies of exosome release by $CD71^+$ cells *in vitro* would provide greater insight into the magnitude of exosome release by these cells as they mature. Further analysis of the exosome release by each of the three layers observed after Percoll separation would give a more nuanced view. Ultimately, the comparison of the release profiles across multiple cell types would give a better sense of scale and an indication of which cell type's exosomes would have the predominant effect in the physiological state. Similarly, profiling the transcriptomes and proteomes of healthy and disease samples in the age of bioinformatics and big data may prove fruitful to precision medicine efforts. Departing from a peripheral blood source for reticulocytes and instead turning towards a hematopoietic progenitor cell source would allow more tailored experiments at different points during erythropoiesis. Profiling exosome release by CD34+ cells as they differentiate towards the erythrocyte has not been done, having relevance not just to peripherally circulating cells but also mechanisms in the bone marrow and the point at which the reticulocyte exits the bone marrow.

In Chapter 5 the potential interactions between reticulocyte-derived exosomes and endothelial cells in regards to vascular function (and dysfunction in pathological states like sickle cell disease) were addressed. The molecular response of endothelial cells to exosomes is the obvious next course of investigation. In the specific case of sickle cell disease, the potential presence of the $\alpha_4\beta_1$ integrin on the surface of sickle reticulocyte-derived exosomes, which has been implicated in the cell adhesion in the vasculature, could further elucidate mechanisms for vaso-occlusion in sickle cell disease. Finally, the troduction of dynamic fluid flow with microfluidic devices is another avenue for investigation. In their native environment of the peripheral circulation, red cells are in

constant motion and *in vitro* experiments that can capture this feature will undoubtedly be more physiologically relevant. An example of a specific study could be an adhesion assay in which endothelial cells that are treated with healthy/sickle reticulocyte-derived exosomes are then exposed to mature sickle red blood cells, as well as white blood cells and platelets and the amount of adhesion of these cells to the endothelial cells recorded and quantified.

Ultimately, the aim is to develop new therapies directed at reticulocyte-driven pathologies. What's envisioned for the continuation of this project is the investigation and harnessing of specific macromolecules (RNAs, proteins) that are differentially expressed in disease-state exosomes. This targeting may be positive or negative—either an attempt to downregulate or upregulate the target molecule. For example, if miR-144 is expressed more in sickle exosomes, then it could be downregulated with an inhibitor, or conversely its downstream target (NRF-2) activated. Since exosomes package such small amounts of macromolecules this route is more appealing than utilizing the exosomes whole.

The major objective of this thesis was to develop a consistent and reliable protocol for the isolation of human peripheral reticulocytes. From there, isolating and characterizing the exosomes released by these cells *in* vitro was done to lay the foundation for more targeted studies investigating the function of these exosomes beyond their role in transferrin receptor clearance during reticulocyte maturation. Ultimately, the completion of these aims is one step closer to uncovering whether unidirectional (or even bidirectional) macromolecule exchange from reticulocytes to endothelial cells modulates endothelial cell function in healthy and disease states.

APPENDIX A. RETICULOCYTE PROTOCOLS

The following protocol details the method for the isolation of $CD71^+$ reticulocytes from human blood. A desired requisite for the publication of this method is that the steps for the reticulocyte isolation procedure will be detailed in narrative form in a non-truncated methodology section and provided in list-style (as seen here) in a supplementary document.

A.1 Cellulose column preparation

This protocol should be executed on the day prior to reticulocyte isolation from whole blood. This protocol was adapted from Venkatesan, 2012.

Materials

- Cellulose, medium fibers (Sigma C6288)
- 10mL centered syringes (BD 309604)
- Whatman grade 105 lens tissue (100 x 150mm, 25 wallets, Whatman 2105-841)
- 15mL and 50mL polypropylene tubes
- 1X PBS (Ca^{2+} & Mg^{2+} free)

Steps

1. Wear a mask to avoid inhalation of cellulose powder. Or work in fume hood.
2. Cut lens tissue into 10mm x 10mm squares.
3. Remove syringe plunger.
4. Use forceps to load two squares into syringe, covering the opening of the syringe.
5. Load cellulose into the barrel, up to ~8mL mark.
6. Reinsert syringe plunger and push cellulose down. Make sure that the top of the cellulose layer is at the ~5.7mL mark on the syringe.

7. Repeat for the number of columns needed. For one 10mL blood sample, 4 columns are needed.
8. Store columns in absorbant packing material at room temperature until use.

A.2 70% Percoll Solution Preparation

All steps must be performed in sterile conditions. It is best to prepare the solution at the very start of the day of reticulocyte isolation so that the Percoll can warm to room temperature prior to its use.

Materials

- Percoll, cell culture-tested (Sigma P4937), 4°C
- 10X PBS
- 1X PBS (Ca^{2+} & Mg^{2+} free), sterile
- Motorized pipettor
- Serological pipets

Steps

1. Prepare "100%" Percoll: Add 9 parts cell-culture tested Percoll to 1 part 10X PBS, depending on desired volume. For example, to make 12mL 100% Percoll: mix 10.8mL Percoll stock and 1.2mL 10X PBS.
2. Add 7 parts 100% Percoll to 3 parts 1X PBS based on desired volume. For example, to make 15mL 70% Percoll: mix 10.5mL 100% Percoll and 4.5mL 1X PBS.
3. Load 15mL tubes with 6mL 70% Percoll.
4. Keep 70% Percoll solution at room temperature.

A.3 Isolation of $CD71^+$ Reticulocytes from Peripheral Blood

Materials

- 10mL blood sample in EDTA vacutainer (purple cap)
- 15mL and 50mL polypropylene tubes
- 2mL cryovials
- 1X PBS (Ca^{2+} & Mg^{2+} free), sterile
- MACS BSA Stock Solution (Miltenyi 130-091-376), 4°C
- autoMACS Rinsing Solution (Miltenyi 130-091-222), RT
- CD71 Beads (Miltenyi 130-046-201), 4°C
- Motorized pipettor & serological pipets
- Micropipettors & tips
- Plastic transfer pipets
- Un- and refrigerated centrifuges with swinging bucket rotor
- autoMACS pro separator + 15mL chill rack
- Cell counter
- T-25 flask
- Reticulocyte culture medium

Prior to Start

1. Prepare MACS Buffer (PBS/0.5% BSA/2mM EDTA) Solution: Dilute MACS BSA Stock Solution 1:20 with autoMACS Rinsing solution (1mL BSA stock + 19 mL Rinsing). Keep at 4°C. Good for 2 weeks.
2. Precool chill rack at 4°C.

Steps

Plasma Removal & Leukocyte and Platelet Depletion

1. Secure cellulose columns into 50mL polypropylene tubes with tape.
2. Load each cellulose column with 6mL 1X PBS. While PBS is traveling through columns proceed to Step 3.
3. Transfer whole blood from vacutainer gently to 15mL polypropylene tube.
4. Centrifuge: 1000g/10 minutes/room temperature (RT)/acceleration:5/no brakes.
5. Use transfer pipets to remove plasma. Aliquot 1mL plasma per cryovial.

6. Dilute packed cell volume to twice the original blood sample volume. For example, for a 10mL blood sample bring volume up to 20mL. This may require transferring sample to 50mL tube.
7. *(only when no PBS is at top of cellulose column)* Load 5mL of diluted blood to each cellulose column. Note: One 10mL blood samples requires four columns.
8. Allow blood to pass through columns (2-3 hours).

70% Percoll Separation

1. Once blood has almost passed through completely, load 5mL 1X PBS into each column.
2. Insert plunger and push rest of solution through the column.
3. Pool samples (usually two 50mL tubes needed) and centrifuge: 1000g/10 minutes/RT/acceleration:5/no brakes.
4. Aspirate PBS. Combine pellets. Bring volume to 10mL. Mix gently with low speeds on motorized pipettor.
5. Layer 5mL blood onto 6mL 70% Percoll cushion with the gravity mode dispense setting on the motorized pipettor. Note: angle tube so that the meniscus of the 70% Percoll is around the 5.2mL mark of 15mL tube, then load blood. Load only one tube at a time. Great care should be taken with this step.
6. Centrifuge: 1200g/15 minutes/RT/acceleration: 5/no brakes (~40 minutes total).
7. Three layers should be observed after centrifugation.
8. Use 1mL micropipettor to aspirate and pool the three layers in a new tube.
9. Add 1X PBS to double the volume of the sample. **Use chilled PBS from now on.**
10. Centrifuge: 300g/10 minutes/4°C/low acceleration/low deceleration.

11. Repeat steps 5-7 for rest of blood sample if applicable.
12. Aspirate three layers and pool with rest of sample.
13. Add chilled 1X PBS to double the volume of the sample.
14. Centrifuge: 300g/10 minutes/4°C/low acceleration/low deceleration.
15. Aspirate PBS. Resuspend sample in 6-8mL fresh, chilled 1X PBS.

For some studies stopping at the point may be sufficient. If not, continue.

$CD71^+$ Immunomagnetic Selection

1. Count cells using the Countess II automated cell counter.
2. Centrifuge: 400g/5 minutes/4°C/low acceleration/low deceleration.
3. Aspirate supernatant. Resuspend pellet in 80µL of MACS Buffer per 10^7 cells. If less than 10^7 cells do not scale down.
4. Add 40µL CD71 beads per 10^7 cells.
5. Mix well and incubate at 4°C for 15 min.
6. After incubation, wash cells by adding 1-2mL MACS Buffer per 10^7 cells.
7. Centrifuge: 400g/5 minutes/4°C/low acceleration/low deceleration.
8. Aspirate supernatant. Resuspend in 500µl MACS Buffer.
9. Run POSSEL program on autoMACs pro separator.
10. Cells in Row C of 15mL chill rack are the $CD71^+$ cells (2mL total volume).
11. Cells in Row B of 15mL chill rack are the CD71- cells (3mL total volume).
12. Count cells from both populations.
13. Store at 4°C or proceed to incubation in reticulocyte medium in T-25 flask (minimum volume 5mL) at 37°C.

A.4 Cytospin Preparation of Reticulocytes

Reticulocytes were usually prepared on cytospin slides within twenty-four hours of their isolation using the following protocol. Prior to their immobilization the slides the cells were stored at 4ºC in 1X PBS. It is essential to filter the brilliant cresyl blue stain prior to its incubation with the cells to avoid the presence of dye aggregates in the images. "Thermo" refers to Thermo Fisher Scientific.

Materials

- Brilliant cresyl blue (Merck 101384)
- EZ single cytofunnels with white cards (Thermo 10-354)
- Cytoslides (Thermo 5991056)
- Funnel Clips (Thermo 10-357)
- 1X PBS (Ca^{2+} & Mg^{2+} free), sterile
- 1.5mL polypropylene tubes (sterile)
- Whatman Grade 1 Filter Paper (Whatman 28413923)
- Reticulocyte culture medium

Prior to start

1. *Prepare Cresyl Blue 1:100 working solution fresh before each use:*
    a. Dilute stock solution of Cresyl Blue 1:100 in 1X PBS.
    b. Filter with Grade 1 filter paper.
2. Prewarm culture medium in 37°C water bath

Steps

1. Aliquot 250,000-500,000 cells from reticulocytes isolated with autoMACS for each cytospin preparation.
2. If alqiout volume greater that 200µL, centrifuge 400g/5 minutes/RT, low acceleration and deceleration, swinging bucket rotor. Resuspend in 100µL 1X PBS.

3. Add equal volume Cresyl Blue working solution to sample. Incubate at RT for 30 minutes.
4. After incubation add 200-300µL warm culture medium. Mix well.
5. Pipette cells into the assembled sample chamber (clip + cytoslide + funnel) (maximum volume for single cytofunnel is 0.5mL).
6. Cytospin samples: 700 rpm/3min/RT, soft spin (acceleration: low, brake: low).
7. Air dry the slides in a vertical position.
8. Examine under microscope.

A.5 Flow Cytometry Analysis of Acridine Orange-Bound RNA

To determine whether the $CD71^+$ cells that were isolated contained RNA, acridine orange staining was performed and the stain detected with flow cytometry.

Materials

- Acridine Orange (AO) (10 mg/mL, Thermo A3568), 4°C; Emission: PerCp-Cy5-5-A, 615-620nm)
- FACS Tubes (12 x 75 mm, capped, BD Falcon 352054)
- 1X PBS (Ca^{2+} & Mg^{2+} free), sterile
- 15 mL polypropylene tubes
- Refrigerated centrifuge
- Aluminum foil

Steps

1. Determine volume of suspension corresponding to 250,000-500,000 cells needed. Aliquot this volume into FACS tube.
2. Balance volume with 1X PBS.
    a. If 250,000 cells stained, bring volume to 0.5mL.
    b. If 500,000 cells stained, bring volume to 1.0mL.

3. Add 1µL of 10 mg/mL AO solution to each FACS tube for RNA staining. Cover with foil.
4. Incubate for 30 minutes at room temperature. Do not wash cells.
5. Analysis must follow immediately.

APPENDIX B. EXOSOME PROTOCOLS

B.1 Protein Quantification of Exosomes

The following protocol was used to prepare an exosome sample for the microBCA assay. The microBCA assay was performed as instructed in the manufacturer's instructions with no adjustments. The standard curve used for protein quantification was fit to a second-order polynomial.

Materials

- 10µL exosome sample
- RIPA Buffer (Thermo 89900)
- Phosphatase Inhibitor Cocktail (Thermo 78420)
- Protease Inhibitor Cocktail (Thermo78430)
- 1X PBS (Ca^{2+} & Mg^{2+} free), sterile
- 1.5mL polypropylene tubes, sterile
- Sonicator bath
- Eppendorf centrifuge

Steps

1. Prepare RIPA Buffer by adding 10µL of each inhibitor cocktail to the 1mL RIPA. Scale up accordingly depending on buffer volume needed.
2. Mix exosome sample with 40µL RIPA Buffer.
3. Sonicate for 15 seconds, three times.
4. Add 400µL 1X PBS to each tube.
5. Centrifuge: 13000g/5 minutes/room temperature.
6. Proceed to microBCA assay.
7. Remember to consider 1/45 dilution of sample when quantifying protein concentration.

B.2 Delivery of Stained Exosomes to Endothelial Cells

Exosomes were stained with the lipophilic dye prior to their incubation with human umbilical vein endothelial cells (HUVECs).

Materials

- Exosome sample (20µg-100µg protein equivalent, 100µL total in 1X PBS)
- Cultured HUVECs
- Reticulocyte culture medium
- HUVEC culture medium
- Polypropylene tubes (sterile): 1.5mL, 15mL, 50mL
- Motorized pipettor & serological pipets, micropipettors & tips
- Cell counter
- Glass bottom microwell dishes (10mm Microwell, Mattek P35G-1.5-10-C)
- BODIPY TR Ceramide (Thermo D7540; fluoresces in red spectrum)
- Exosome spin columns (Thermo 4484449)
- 10% neutral-buffered formalin (Fisher 23-245684)
- 1X PBS (Ca^{2+} & Mg^{2+} free), sterile
- DAPI-FluoroMount-G (Southern Biotech 0100-20)
- Coverslips
- Confocal or wide-field microscope

Steps

Day Prior to Exosome Staining & Delivery

1. Culture HUVECs in plastic flasks (T25s or T75s) to 75-80% coverage of flask.
2. Coat microwell dishes with 1% gelatin. 250µL is sufficient for 10mm glass insert.
3. Aspirate gelatin. Add 1ml prewarmed HUVEC medium to microwell dishes (to prime dishes). Incubate at 37°C.
4. Harvest cells from plastic flasks. Count.
5. Seed 2500-5000 cells onto 10mm glass insert. Incubate at 37°C for 1 hour.
6. After 1 hour add additional HUVEC medium to bring final volume in dish to 2.5ml.

Exosome Staining & Delivery

1. Prepare 1mM BODIPY solution: Resuspend powder in 354.25µL DMSO. Make aliquots of stock. Store all tubes at -20°C. Protect all tubes from light.
2. Add 1µL BODIPY stock solution to exosome sample to achieve 10µM treatment concentration. Control: Add 1µL BODIPY stock solution to 1X PBS.
3. Incubate for 20 minutes/37ºC in dark.
4. Remove unbound dye with exosome spin column (follow manufacturer's instructions for preparation of column).
5. Incubate stained exosomes or control with HUVECs for 2 hours.
6. After incubation period, aspirate medium.
7. Wash ECs with warm PBS once.
8. Fix ECs with 10% neutral buffered formalin; 1mL formalin/dish. Incubate at RT for 15 minutes.
9. Rinse 3X in PBS.
10. Mount with DAPI-FluoroMount-G and put coverslip on sample.
11. Observe samples with fluorescence microscopy.

APPENDIX C. CELL CULTURE & RNA PROTOCOLS

C.1 Reticulocyte & K562 Culture Medium

The following medium formulation (Table C1) was used to culture K562 cells, as well as for the incubation of reticulocytes isolated from peripheral blood.

Table C1 – Supplies needed to prepare medium.

Component	Vendor/Cat#	Quantity	Formulation	Final Conc.
RPMI 1640 (1X) medium	Life Technologies (Invitrogen)/ 11875093	500mL	Supplemented with l-glutamine (2mM), no HEPES	-
Fetal bovine serum (FBS)	Gibco/ A2720801 Lot: FB11554HI	500mL	Exosome-depleted	10% v/v
Pen/Strep	Mediatech/ 30-002-CI	100mL	10K U/mL Penicillin 10K µg/mL Streptomycin	50 U/mL Pen 50 µg/mL Strep
Filtration unit	ThermoFisher/ 166-0045	500mL unit	-	-

Step

1. Combine components in the amounts in Table C2 to produce 500 mL of medium.

2. 0.2µm filter the medium into a sterile 500 ml bottle. The volumes can be scaled accordingly.

3. Store medium at 4ºC for up to one month.

Table C2 – Combination of medium components.

Component	Volume	Storage
RPMI	447.5mL	4°C
Exosome-free FBS	50mL	-20°C
Pen/Strep	2.5mL	-20°C

C.2 Plating Endothelial Cells from Frozen Vials into T-75 Flasks

Materials

- T75 flask(s), pre-coated with 1% gelatin
- Cell culture medium
- Assorted sterile pipettes (1mL, 5mL, 10mL, 25mL)

Steps

1. Calculate the volume of culture medium that needs to be prepared:
    a. Add 15 mL culture medium directly to each T75 flask to be seeded, label and date flask, place in incubator for 30 minutes to equilibrate;
    b. Add 5 mL to a 15 mL tube which will be used to suspend cells from pellet, place in water bath. Prepare separate tube for each vial to be plated.
2. At 20-25 minutes into equilibration of flasks, retrieve vials of cells from liquid N2 storage.
3. Thaw frozen vial by hand in water bath just until last bit of ice has melted, do not allow it to remain in the bath any longer.
4. Transfer contents of thawed vial to tube containing warm culture medium, invert 2-3 times to mix.

5. Retrieve T75 flask(s) from incubator, transfer cell suspension to flask(s) dividing as necessary. Try not to exceed 2500 cells/cm^2 recommended seeding density. Return flasks to incubator.
6. Replace culture medium in newly seeded flask on the next day to limit exposure of cells to DMSO in cryopreservation medium.
7. Continue to culture endothelial cells until they cover 75-80% of the flask surface, usually 3-4 days.
8. Subculture cells using the Lonza Subculture ReagantPack (Cat# CC-5034) and maintain 2500 cells/cm^2 seeding density in subsequent flasks.

C.3 TaqMan Reverse Transcription

Materials

- Purified RNA (stored at -80°C)
- Polypropylene microcentrifuge tubes (1.5 mL, sterile)
- TaqMan MicroRNA Reverse Transcription Kit (RT) (Life Technologies 4366596, 200 reactions, stored at -20°C)
- 5X RT Primer from TaqMan MicroRNA Assays, stored at -20°C
- miR144 - Life Technologies 4427975/ID 002676, 50 reactions
- TaqMan assays for housekeeping genes
- Microcentrifuge, pre-chilled to 4°C
- Nuclease-free water (stored at room temperature)

Steps

1. Wipe down bench area with 10% bleach prior to start.
2. Allow the purified RNA, TaqMan® MicroRNA Reverse Transcription Kit components, and 5X RT Primer to thaw on ice.
3. Aliquot nuclease-free water (e.g. 1 mL in a microcentrifuge tube) and chill on ice.
4. Centrifuge tubes to bring solutions to the bottom of the tubes.

5. Determine volume of RNA to be added (**1-500ng**).
6. In a 1.5-mL polypropylene tube, prepare the RT master mix on ice by scaling the volumes listed in Table C3 to the desired number of RT reactions. Add 0.5X for overage i.e., for 10 samples multiply all volumes by 10.5**.** Adding 10 to 20% overage accounts for pipetting losses.

Table C3 – Reagants volumes for RT master mix.

Component	Master mix volume per 15µL reaction
100mM dNTPs (with dTTP)	0.15µL
MultiScribe™ Reverse Transcriptase, 50U/µL	1.00µL
10× Reverse Transcription Buffer	1.50µL
RNase Inhibitor, 20U/µL	0.19µL
Nuclease-free water	4.16µL
Total	**7.00µL**

7. Create each 15µL RT reaction with:
    a. 7µL RT Master Mix
    b. Determined volume of RNA.
    c. 3µL of 5× RT primer from each assay set into the corresponding RT reaction tube.
    d. Balance with nuclease-free water to 15µL.
8. Mix gently, then centrifuge briefly.
9. Transfer 15µL solution into a 0.2-mL polypropylene reaction tube.
10. Incubate the tube on ice for 5 minutes and keep it on ice until ready to load the thermal cycler.

11. Use the following stages (in order of occurrence) to program the thermal cycler:

    a. 30 minutes/16ºC

    b. 30 minutes/42ºC

    c. 5 minutes/85ºC

    d. Infinite/4ºC

12. Set the reaction volume to 15.0µL.

13. Load the reaction tube or plate into the thermal cycler.

14. Start the RT run.

15. If you do not immediately continue to PCR amplification after the RT run, store the RT reaction at −15 to −25°C.

C.4 TaqMan qPCR

Materials

- Purified cDNA (stored at -20°C)
- Polypropylene microcentrifuge tubes (1.5 mL, autoclaved)
- TaqMan MicroRNA Assay 20X (stored at -20°C)
- miR144 - Life Technologies 4427975/ID 002676, 150 rxns
- TaqMan assays for housekeeping genes
- TaqMan Universal PCR Master Mix II 2X, no UNG, 200 rxns (Life Technologies 4440040, stored at 4°C)
- Microcentrifuge, pre-chilled to 4°C
- Optical adhesive covers (Applied Biosystems 4360954)

Steps

Prepare qPCR reaction mix

1. Allow the purified cDNA and TaqMan® MicroRNA Assays to thaw on ice. Protect the MicroRNA Assays from light with aluminum foil.

2. Aliquot nuclease-free water (e.g. 1 mL in a microcentrifuge tube) and chill on ice.

3. Centrifuge tubes to bring solutions to the bottom of the tubes.

4. Obtain a 1.5-mL polypropylene tube for each sample.
5. Prepare the qPCR reaction mix on ice by scaling the volumes listed in Table C4 to at least three replicates of each sample including the no template controls. Make 3.5X for overage. Adding 10 to 20% overage accounts for pipetting losses.
6. Invert solution several times to mix. Then centrifuge briefly.

Table C4 – qPCR reaction mix components.

Component	Rxn mix volume per 20-µl reaction
TaqMan Small RNA Assay (20X)	1.00µL
Product from RT reaction	1.00µL (1.33µL - max)
TaqMan Universal PCR Master Mix (2X), no UNG	10.00µL
Nuclease-free water	8.00µL
Total	**20.00µL**

Prepare and run PCR reaction plate

1. Transfer 20µL of the complete qPCR reaction mix (including assay and RT product) into each of three wells on a 48-, 96-, or 384-well plate. Make note of sample placement in plate.
2. Seal the plate with the optical cover to avoid evaporation of samples.
3. Centrifuge the plate briefly if necessary.
4. Load the plate into the instrument.
5. Run the PCR System with the following parameters:
    a. Run Mode: Standard
    b. Sample Volume: 20µL
    c. Thermal cycling conditions in Table C5

Table C5 -- qPCR thermal cycling conditions.

Step	Enzyme Activation	PCR	
	HOLD	CYCLE (40 cycles)	
		Denature	Anneal/extend
Temperature	95°C	95°C	60°C
Time	10 minutes	15 seconds	60 seconds

6. Start the PCR run.

APPENDIX D. R CODE USED TO PERFORM STATISTICS

The following lines of codes were executed in the software R to perform statistics on the protein and exosome quantification data. R was chosen over Excel because it offers greater freedom in defining the test parameters. For example, changing the confidence level of the statistical tests was possible, which was necessary for computing the p-value of the 97.5% confidence level t-test in the flow cytometry analysis.

Figure D1 shows the code used to test the difference between the mean protein concentrations for K562 (n=5) and reticulocyte exosomes (n=3). The comments (in green) are annotations to what the code is doing. First, an F test was used to test the homoscedasticity of the two populations. The result of that test influenced the "var.equal" parameter in the call to the t.test function. Two t-tests were performed: a one-tailed test determining whether the difference between the means (K562 exosomes minus reticulocyte exosomes) was greater than 0 and a two-tailed test determining whether the difference between the means was not equal to 0. The two-tailed tests is usually what is output to Excel and the p-value and test statistics are reported in Chapter 5. Both tests returned p-values less than 0.05, indicating a significant difference between the mean protein concentrations of the populations.

Similarly, Figure D2 shows the R code use to compare the difference between the mean exosome number for each of the populations. The p-values for both t-tests in this case were greater than 0.05, indicating no significant difference between the mean exosome count for each 5µg protein equivalent of each sample.

```r
##Comparing mean protein concentration of the five K562 samples used in ExoELISA

cd71pos <- c(200.5284258, 235.7533495, 230.917137)
k562 <- c(400.8610809,215.4833776,506.1878117,384.768141,498.5369871)

#Test equality of variances using two-sided F test, alpha = .05
#null: ratio of variances = 1; alternative: ration of variances ~= 1
var.test(cd71pos, k562)
#p-value = 0.05176 > .05, accept null, equal variances


#Perform one-tailed t test, alpha = .05
#null: mu_k562 - mu_cd71pos = 0; alternative: mu_k562 - mu_cd71pos > 0
t.test(k562, cd71pos, mu=0, alternative = "g", paired = FALSE, var.equal = TRUE, conf.level = .95)
#p-value = 0.02222, reject null, t-statistic = 2.5341

#Perform two-tailed t test, alpha = .05
#null: mu_k562 - mu_cd71pos = 0; alternative: mu_k562 - mu_cd71pos ~= 0
t.test(k562, cd71pos, mu=0, alternative = "t", paired = FALSE, var.equal = TRUE, conf.level = .95)
#p-value = 0.04443 < .05, reject null, t-statistic = 2.5341
```

Figure D1 – R code testing difference between mean protein concentrations.

```r
##Comparing mean exosome number for the 5 K562 samps & 3 cd71pos samps (5ug) used in the ExoELISA

cd71pos <- c(9.265E+09,1.695E+10,8.122E+10)
k562 <- c(2.076E+10,6.546E+10,9.339E+10,9.458E+10,8.717E+10)

#Test equality of variances using two-sided F test, alpha = .05
#null: ratio of variances = 1; alternative: ration of variances ~= 1
var.test(cd71pos, k562)
#p-value = 0.612 > .05, accept null, equal variances


#Perform one-tailed t test, alpha = .05
#null: mu_k562 - mu_cd71pos = 0; alternative: mu_k562 - mu_cd71pos > 0
t.test(k562, cd71pos, mu=0, alternative = "g", paired = FALSE, var.equal = TRUE, conf.level = .95)
#p-value = 0.09691, accept null, t-statistic = 1.4629

#Perform two-tailed t test, alpha = .05
#null: mu_k562 - mu_cd71pos = 0; alternative: mu_k562 - mu_cd71pos ~= 0
t.test(k562, cd71pos, mu=0, alternative = "t", paired = FALSE, var.equal = TRUE, conf.level = .95)
#p-value = 0.1938 > .05, accept null, t-statistic = 1.4629
```

Figure D2 – R code testing difference between mean exosome counts (5µg samples).

Figure D3 shows the code used to test the difference between the "exosome release potential" profiles of the K562 and reticulocyte exosomes. The protein concentration per exosome between the two groups was not significantly different, as indicated by the two t-tests performed. This result suggests that on average the cells release a comparable number of exosomes, that also have a comparable average amount of total protein. However, in absolute terms there are about twice as many K562

exosomes per protein microgram equivalent of samples when dividing the average values in Figure 31.

```
##Comparing protein concen./exosome number for the 5 K562 samp & 3 cd71pos samps (10ul) used in the ExoELISA

cd71pos <- c(4.39E-08,4.37E-08,3.67E-09)
k562 <- c(1.11614E-08,6.57362E-09,4.89023E-09,4.14398E-09,5.52855E-09)

#Test equality of variances using two-sided F test, alpha = .05
#null: ratio of variances = 1; alternative: ration of variances ~= 1
var.test(cd71pos, k562)
#p-value = 0.001557 < .05, reject null, unequal variances


#Perform one-tailed t test, alpha = .05
#null: mu_k562 - mu_cd71pos = 0; alternative: mu_k562 - mu_cd71pos > 0
t.test(k562, cd71pos, mu=0, alternative = "g", paired = FALSE, var.equal = FALSE, conf.level = .95)
#p-value = 0.893, accept null, t-statistic = -1.784

#Perform two-tailed t test, alpha = .05
#null: mu_k562 - mu_cd71pos = 0; alternative: mu_k562 - mu_cd71pos ~= 0
t.test(k562, cd71pos, mu=0, alternative = "t", paired = FALSE, var.equal = FALSE, conf.level = .95)
#p-value = 0.2143 > .05, accept null, t-statistic = -1.784
```

Figure D3 – R code testing difference between mean exosome counts (10µL samples).

REFERENCES

Almeida, A. & Roberts, I. Bone involvement in sickle cell disease. *British Journal of Haematology* **129**, 482-490 (2005).

Applied Biosystems. Endogenous Controls for Real-Time Quantitation of miRNA Using TaqMan® MicroRNA Assays. . (2010). Available at: http://tools.thermofisher.com/content/sfs/brochures/cms_044972.pdf. (Accessed: 4th February 2017).

Ballas, S. & Smith, E. Red blood cell changes during the evolution of the sickle cell painful crisis. *Blood* **79**, 2154-2163 (1992).

Barabino, G., McIntire, L., Eskin, S., Sears, D. & Udden, M. Endothelial cell interactions with sickle cell, sickle trait, mechanically injured, and normal erythrocytes under controlled flow. *Blood* **70**, 152-157 (1987).

Barabino, G.A., Platt, M.O. & Kaul, D.K. Sickle Cell Biomechanics. *Annual Review of Biomedical Engineering* **12**, 345-367 (2010).

Barrès, C. et al. Galectin-5 is bound onto the surface of rat reticulocyte exosomes and modulates vesicle uptake by macrophages. *Blood* **115**, 696-705 (2010).

Belcher, J.D., Marker, P.H., Weber, J.P., Hebbel, R.P. & Vercellotti, G.M. Activated monocytes in sickle cell disease: potential role in the activation of vascular endothelium and vaso-occlusion. *Blood* **96**, 2451-2459 (2000).

Blanc, L., De Gassart, A., Géminard, C., Bette-Bobillo, P. & Vidal, M. Exosome release by reticulocytes—An integral part of the red blood cell differentiation system. *Blood Cells, Molecules, and Diseases* **35**, 21-26 (2005).

Blanc, L., Barres, C., Bette-Bobillo, P. & Vidal, M. Reticulocyte-secreted exosomes bind natural IgM antibodies: involvement of a ROS-activatable endosomal phospholipase iPLA2. *Blood* **110**, 3407-3416 (2007).

Blanc, L. et al. The water channel aquaporin-1 partitions into exosomes during reticulocyte maturation: implication for the regulation of cell volume. *Blood* **114**, 3928 (2009).

Bonauer, A., Boon, R.A. & Dimmeler, S. Vascular microRNAs. *Current Drug Targets* **11**, 943-949 (2010).

Bonauer, A., Boon, R.A. & Dimmeler, S. Vascular microRNAs. *Current Drug Targets* **11**, 943-949 (2010).

Bruchova-Votavova, H., Yoon, D. & Prchal, J.T. miR-451 enhances erythroid differentiation in K562 cells. *Leukemia & Lymphoma* **51**, 686-693 (2010).

Brun, A., Gaudernack, G. & Sandberg, S. A new method for isolation of reticulocytes: positive selection of human reticulocytes by immunomagnetic separation. *Blood* **76**, 2397-2403 (1990).

Carayon, K. et al. Proteolipidic Composition of Exosomes Changes during Reticulocyte Maturation. *Journal of Biological Chemistry* **286**, 34426-34439 (2011).

Chen, S.-Y., Wang, Y., Telen, M.J. & Chi, J.-T. The Genomic Analysis of Erythrocyte microRNA Expression in Sickle Cell Diseases. *PLoS ONE* **3**, e2360 (2008).

Chen, X.-L. et al. Activation of Nrf2/ARE pathway protects endothelial cells from oxidant injury and inhibits inflammatory gene expression. *American Journal of Physiology-Heart and Circulatory Physiology* **290**, H1862-H1870 (2006).

Cheng, X., Ku, C.-H. & Siow, R. Regulation of the Nrf2 antioxidant pathway by microRNAs: New players in micromanaging redox homeostasis. *Free Radical Biology and Medicine* (2013).

Cho, J.-S. et al. Unambiguous determination of Plasmodium vivax reticulocyte invasion by flow cytometry. *International Journal for Parasitology* **46**, 31-39 (2016).

Davidson, B.L. & McCray, P.B. Current prospects for RNA interference-based therapies. *Nat Rev Genet* **12**, 329-340 (2011).

De Toro, J., Herschlik, L., Waldner, C. & Mongini, C. Emerging Roles of Exosomes in Normal and Pathological Conditions: New Insights for Diagnosis and Therapeutic Applications. *Frontiers in Immunology* **6** (2015).

Denzer, K., Kleijmeer, M.J., Heijnen, H.F., Stoorvogel, W. & Geuze, H.J. Exosome: from internal vesicle of the multivesicular body to intercellular signaling device. *Journal of Cell Science* **113**, 3365-3374 (2000).

Douay, L. & Giarratana, M.-C. in Stem Cells in Regenerative Medicine 127-140 (Springer, 2009).

Frank, M.G., Wieseler-Frank, J.L., Watkins, L.R. & Maier, S.F. Rapid isolation of highly enriched and quiescent microglia from adult rat hippocampus: Immunophenotypic and functional characteristics. *Journal of Neuroscience Methods* **151**, 121-130 (2006).

Franquesa, M. et al. Update on Controls for Isolation and Quantification Methodology of Extracellular Vesicles Derived from Adipose Tissue Mesenchymal Stem Cells. *Frontiers in Immunology* **5** (2014).

Gee, B. & Platt, O. Sickle reticulocytes adhere to VCAM-1. *Blood* **85**, 268-274 (1995).

Giarratana, M.-C. et al. Ex vivo generation of fully mature human red blood cells from hematopoietic stem cells. *Nat Biotech* **23**, 69-74 (2005).

Griffiths, R.E. et al. Maturing reticulocytes internalize plasma membrane in glycophorin A–containing vesicles that fuse with autophagosomes before exocytosis. *Blood* **119**, 6296-6306 (2012).

Griffiths, R.E. et al. The ins and outs of human reticulocyte maturation: Autophagy and the endosome/exosome pathway. *Autophagy* **8**, 1150-1151 (2012).

Harding, C., Heuser, J. & Stahl, P. Receptor-mediated endocytosis of transferrin and recycling of the transferrin receptor in rat reticulocytes. *The Journal of cell biology* **97**, 329-339 (1983).

Hata, A. Functions of MicroRNAs in Cardiovascular Biology and Disease. *Annual Review of Physiology* **75**, 69-93 (2013).

Hergenreider, E. et al. Atheroprotective communication between endothelial cells and smooth muscle cells through miRNAs. *Nat Cell Biol* **14**, 249-256 (2012).

Hu, J. et al. Isolation and functional characterization of human erythroblasts at distinct stages: implications for understanding of normal and disordered erythropoiesis in vivo. *Blood* **121**, 3246-3253 (2013).

Hunter, M.P. et al. Detection of microRNA Expression in Human Peripheral Blood Microvesicles. *PLOS ONE* **3**, e3694 (2008).

Iguchi, H., Kosaka, N. & Ochiya, T. Secretory microRNAs as a versatile communication tool. *Communicative & Integrative Biology* **3**, 478-481 (2010).

Jahanmehr, S.A., Hyde, K., Geary, C.G., Cinkotai, K.I. & Maciver, J.E. Simple technique for fluorescence staining of blood cells with acridine orange. *Journal of Clinical Pathology* **40**, 926-929 (1987).

Johnstone, R.M. Exosomes biological significance: A concise review. *Blood Cells, Molecules, and Diseases* **36**, 315-321 (2006).

Johnstone, R.M., Adam, M., Hammond, J.R., Orr, L. & Turbide, C. Vesicle formation during reticulocyte maturation. Association of plasma membrane activities with released vesicles (exosomes). *Journal of Biological Chemistry* **262**, 9412-9420 (1987).

Johnstone, R.M., Mathew, A., Mason, A.B. & Teng, K. Exosome formation during maturation of mammalian and avian reticulocytes: Evidence that exosome release is a major route for externalization of obsolete membrane proteins. *Journal of Cellular Physiology* **147**, 27-36 (1991).

Joneckis, C., Ackley, R., Orringer, E., Wayner, E. & Parise, L. Integrin alpha 4 beta 1 and glycoprotein IV (CD36) are expressed on circulating reticulocytes in sickle cell anemia. *Blood* **82**, 3548-3555 (1993).

Kaul, D.K., Fabry, M.E., Windisch, P., Baez, S. & Nagel, R.L. Erythrocytes in sickle cell anemia are heterogeneous in their rheological and hemodynamic characteristics. *The Journal of clinical investigation* **72**, 22-31 (1983).

Kikuchi-Taura, A., Soma, T., Matsuyama, T., Stern, D.M. & Taguchi, A. A New Protocol for Quantifying CD34+ Cells in Peripheral Blood of Patients with Cardiovascular Disease. *Texas Heart Institute Journal* **33**, 427-429 (2006).

Kosaka, N. et al. Secretory mechanisms and intercellular transfer of microRNAs in living cells. *Journal of Biological Chemistry* **285**, 17442-17452 (2010).

Koury, M.J., Koury, S.T., Kopsombut, P. & Bondurant, M.C. In vitro maturation of nascent reticulocytes to erythrocytes. *Blood* **105**, 2168-2174 (2005).

Kroh, E.M., Parkin, R.K., Mitchell, P.S. & Tewari, M. Analysis of circulating microRNA biomarkers in plasma and serum using quantitative reverse transcription-PCR (qRT-PCR). *Methods* **50**, 298-301 (2010).

Kumar, A.A. et al. Enrichment of reticulocytes from whole blood using aqueous multiphase systems of polymers. *American Journal of Hematology* **90**, 31-36 (2015).

Latronico, M.V.G., Catalucci, D. & Condorelli, G. Emerging Role of MicroRNAs in Cardiovascular Biology. *Circulation Research* **101**, 1225-1236 (2007).

Lew, V.L. & Bookchin, R.M. Ion Transport Pathology in the Mechanism of Sickle Cell Dehydration. *Physiological Reviews* **85**, 179-200 (2005).

Lopez, B.L., Griswold, S.K., Navek, A. & Urbanski, L. The Complete Blood Count and Reticulocyte Count–Are They Necessary in the Evaluation of Acute Vasoocclusive Sickle-cell Crisis? *Academic Emergency Medicine* **3**, 751-757 (1996).

Lozzio, C. & Lozzio, B. Human chronic myelogenous leukemia cell-line with positive Philadelphia chromosome. *Blood* **45**, 321-334 (1975).

Makis, A., Hatzimichael, E. & Bourantas, K. The role of cytokines in sickle cell disease. *Annals of hematology* **79**, 407-413 (2000).

Malleret, B. et al. Plasmodium vivax: restricted tropism and rapid remodeling of CD71-positive reticulocytes. *Blood* **125**, 1314-1324 (2015).

Martin-Jaular, L., Nakayasu, E.S., Ferrer, M., Almeida, I.C. & del Portillo, H.A. Exosomes from Plasmodium yoelii-Infected Reticulocytes Protect Mice from Lethal Infections. *PLOS ONE* **6**, e26588 (2011).

Moreno- Pérez, D.A., Ruíz, J.A. & Patarroyo, M.A. Reticulocytes: Plasmodium vivax target cells. *Biology of the Cell* **105**, 251-260 (2013).

Ney, P.A. Normal and disordered reticulocyte maturation. *Current opinion in hematology* **18**, 152 (2011).

Noulin, F. et al. Hematopoietic Stem/Progenitor Cell Sources to Generate Reticulocytes for Plasmodium vivax Culture. *PLoS ONE* **9**, e112496 (2014).

Pan, B.-T. & Johnstone, R. M. Fate of the transferrin receptor during maturation of sheep reticulocytes in vitro: Selective externalization of the receptor. *Cell* **33**, 967-978 (1983).

Pan, B.-T., Teng, K., Wu, C., Adam, M. & Johnstone, R. M. Electron microscopic evidence for externalization of the transferrin receptor in vesicular form in sheep reticulocytes. *The Journal of Cell Biology* **101**, 942-948 (1985).

Paszkiet, B. *et al.* Development of an improved process for the depletion of exosomes from fetal bovine serum. (2016). Available at: https://www.thermofisher.com/content/dam/LifeTech/global/life-sciences/CellCultureandTransfection/pdfs/COL11127-ExosomeDepletedFBS-ScientificPoster-updated2016.pdf. (Accessed 4th February 2017).

Pauling, L. & Itano, H.A. Sickle cell anemia a molecular disease. *Science (New York, N.Y.)* **110**, 543-548 (1949).

Platt, O.S. et al. Mortality in sickle cell disease--life expectancy and risk factors for early death. *New England Journal of Medicine* **330**, 1639-1644 (1994).

Ponka, P. & Lok, C.N. The transferrin receptor: role in health and disease. *The International Journal of Biochemistry & Cell Biology* **31**, 1111-1137 (1999).

Ramachandran, S. & Palanisamy, V. Horizontal transfer of RNAs: exosomes as mediators of intercellular communication. *Wiley Interdisciplinary Reviews: RNA* **3**, 286-293 (2012).

Rees, D.C., Williams, T.N. & Gladwin, M.T. Sickle-cell disease. *The Lancet* **376**, 2018-2031 (2010).

Rieu, S., Géminard, C., Rabesandratana, H., Sainte-Marie, J. & Vidal, M. Exosomes released during reticulocyte maturation bind to fibronectin via integrin α4β1. *European Journal of Biochemistry* **267**, 583-590 (2000).

Riley, R.S., Ben-Ezra, J.M., Goel, R. & Tidwell, A. Reticulocytes and reticulocyte enumeration. *Journal of Clinical Laboratory Analysis* **15**, 267-294 (2001).

Roberts, T.C., Coenen-Stass, A.M. & Wood, M.J. Assessment of RT-qPCR normalization strategies for accurate quantification of extracellular microRNAs in murine serum. *PLoS One* **9**, e89237 (2014).

Rushing, D. & Vengelen-Tyler, V. Evaluation and comparison of four reticulocyte enrichment procedures. *Transfusion* **27**, 86-89 (1987).

Russell, B. et al. A reliable ex vivo invasion assay of human reticulocytes by Plasmodium vivax. *Blood* **118**, e74-e81 (2011).

Sangokoya, C., Telen, M.J. & Chi, J.-T. microRNA miR-144 modulates oxidative stress tolerance and associates with anemia severity in sickle cell disease. *Blood* **116**, 4338-4348 (2010).

Savina, A., Furlán, M., Vidal, M. & Colombo, M.I. Exosome release is regulated by a calcium-dependent mechanism in K562 cells. *Journal of Biological Chemistry* **278**, 20083-20090 (2003).

Sharma, R. & Marwaha, N. Leukoreduced blood components: Advantages and strategies for its implementation in developing countries. *Asian Journal of Transfusion Science* **4**, 3 (2010).

Sieff, C. et al. Changes in cell surface antigen expression during hemopoietic differentiation. *Blood* **60**, 703-713 (1982).

Simons, M. & Raposo, G. Exosomes–vesicular carriers for intercellular communication. *Current Opinion in Cell Biology* **21**, 575-581 (2009).

Skadberg, Ø., Brun, A. & Sandberg, S. Human reticulocytes isolated from peripheral blood: maturation time and hemoglobin synthesis. *Laboratory Hematology* **9**, 198-206 (2003).

Small, E.M. & Olson, E.N. Pervasive roles of microRNAs in cardiovascular biology. *Nature* **469**, 336-342 (2011).

Sorette, M., Shiffer, K. & Clark, M. Improved isolation of normal human reticulocytes via exploitation of chloride-dependent potassium transport. *Blood* **80**, 249-254 (1992).

Steinberg, M.H. Sickle cell anemia, the first molecular disease: overview of molecular etiology, pathophysiology, and therapeutic approaches. *The Scientific World Journal* **8**, 1295-1324 (2008).

Stoorvogel, W. Functional transfer of microRNA by exosomes. *Blood* **119**, 646-648 (2012).

Styles, L.A. et al. Decrease of Very Late Activation Antigen-4 and CD36 on Reticulocytes in Sickle Cell Patients Treated With Hydroxyurea. *Blood* **89**, 2554-2559 (1997).

Swerlick, R., Eckman, J., Kumar, A., Jeitler, M. & Wick, T. Alpha 4 beta 1-integrin expression on sickle reticulocytes: vascular cell adhesion molecule-1-dependent binding to endothelium. *Blood* **82**, 1891-1899 (1993).

Tao, Z.-Y., Xia, H., Cao, J. & Gao, Q. Development and evaluation of a prototype non-woven fabric filter for purification of malaria-infected blood. *Malaria Journal* **10**, 1 (2011).

Théry, C., Amigorena, S., Raposo, G. & Clayton, A. in Current Protocols in Cell Biology (John Wiley & Sons, Inc., 2001).

Théry, C., Zitvogel, L. & Amigorena, S. Exosomes: composition, biogenesis and function. *Nature Reviews Immunology* **2**, 569-579 (2002).

Tsiftsoglou, A., Wong, W., Tsamadou, A. & Robinson, S. Cooperative effects of hemin and anthracyclines in promoting terminal erythroid maturation in K562 human erythroleukemia cells. *Experimental Hematology* **19**, 928 (1991).

Valadi, H. et al. Exosome-mediated transfer of mRNAs and microRNAs is a novel mechanism of genetic exchange between cells. *Nat Cell Biol* **9**, 654-659 (2007).

van der Meer, A.D., Poot, A.A., Duits, M.H.G., Feijen, J. & Vermes, I. Microfluidic Technology in Vascular Research. *Journal of Biomedicine and Biotechnology* **2009** (2009).

Venkatesan, M. et al. Using CF11 cellulose columns to inexpensively and effectively remove human DNA from Plasmodium falciparum-infected whole blood samples. *Malaria Journal* **11**, 1-7 (2012).

Vidal, M. Exosomes in erythropoiesis. *Transfusion Clinique et Biologique* **17**, 131-137 (2010).

Wagner, G.M., Chiu, D.T.-Y., Yee, M.C. & Lubin, B.H. Red cell vesiculation—a common membrane physiologic event. *Journal of Laboratory & Clinical Medicine* **108**, 315-324 (1986).

World Health Organization. Sickle-cell disease and other haemoglobin disorders. (2014). Available at: http://www.who.int/mediacentre/factsheets/fs308/en/index.html. (Accessed 4th February 2017).

Zhang, Y. et al. Secreted Monocytic miR-150 Enhances Targeted Endothelial Cell Migration. *Molecular Cell* **39**, 133-144 (2010).

Zhang, Y. et al. Secreted Monocytic miR-150 Enhances Targeted Endothelial Cell Migration. *Molecular Cell* **39**, 133-144 (2010).

Zucker, R.M. & Cassen, B. The separation of normal human leukocytes by density and classification by size. *Blood* **34**, 591-600 (1969).